Combustion Performance of Waste-Derived Fuels with respect to Ultra Low Sulfur Diesel in a Compression Ignition Engine

BY

Preetham Reddy Churkunti

Submitted to the graduate degree program in the Department of Mechanical Engineering and the Graduate Faculty of the University of Kansas in partial fulfillment of the requirements for the degree of Master of Science.

_____

Chair: Dr. Christopher Depcik

_____

Dr. Sarah L Kieweg

_____

Dr. Edward Peltier

Defended: June 15th, 2015

The Thesis Committee for Preetham Reddy Churkunti certifies that this is the approved version of the following thesis:

Combustion Performance of Waste-Derived Fuels with respect to Ultra Low Sulfur Diesel in a Compression Ignition Engine

BY

Preetham Reddy Churkunti

_____

Chair: Dr. Christopher Depcik

Accepted: June 16th, 2015

Abstract

The ever increasing energy demand along with fast depleting non-renewable fossil fuels and global climate change has led to a search for sustainable energy resources. Fuels produced from waste, like plastic solid waste and waste cooking oil, have gained significant interest since they not only solve disposal problems but also provide a sustainable energy resource. This thesis contains detailed literature surveys, combustion analysis of a waste plastic fuel, life cycle analysis of waste plastic fuel and waste cooking oil biodiesel from well to exhaust, and optimization of combustion of waste cooking oil biodiesel by employing higher injection pressures and normalized injection timings in comparison to commercial ultra low sulfur diesel fuel (ULSD).

Chapter 1 introduces the research work with the motivation behind the efforts. In addition, there is a brief discussion on prior and parallel work performed in the employed engine test cell. Moreover, this chapter describes the focus of each chapter with novel and unique findings highlighted.

Chapter 2 describes a literature review to better understand the influence of fuel synthesis technique on fuel properties of waste plastic fuels. Moreover, this chapter contains a combustion analysis of waste plastic fuel blends with ULSD in order to compare performance and emission characteristics of a commercial waste plastic fuel with that of ULSD.

Chapter 3 starts with a literature review to give background on the life cycle analysis and different approaches taken by previous researchers to perform life cycle analysis. This is followed by a well-to-exhaust analysis (WtE) of waste cooking oil biodiesel and waste plastic fuel at full load in comparison to ULSD.

Chapter 4 details the literature review to understand general and specific findings on the influence of injection parameters on the performance and emission characteristics of compression ignition fuels. This chapter contains a detailed combustion analysis of waste cooking oil biodiesel at higher injection pressures and normalized injection timings to attempt to replicate the performance of ULSD by negating the relatively high viscosity of the test fuel.

Chapter 5 summarizes major findings of this work in stages and connects the outcome of efforts to achieve optimal combustion of waste-derived fuels. Furthermore, future efforts are suggested to move towards sustainable public transportation in and around the University of Kansas campus.

Acknowledgements

This work was made possible by the guidance of Dr. Christopher Depcik of the Department of Mechanical Engineering. Furthermore, assistance from Dr. Edward Peltier (of the Department of Civil, Environmental, and Architectural Engineering), as well as advice and support from Jonathan Mattson (of the Department of Mechanical Engineering), greatly aided in the progress and completion of the study in time. Finally, the assistance and experience of Saud Shah Alam and Chenaniah Langness proved to be invaluable in the creation of this work.

Contents

List of Figures

List of Tables

Nomenclature

BSFC	Brake Specific Fuel Consumption
BSE	Brake Specific Emissions
BTE	Brake Thermal Efficiency
CO	Carbon monoxide
CO_2	Carbon dioxide
CH_4	Methane
CX	C (Cyndiesel) X (blend percentage)
ECU	Electronic Control Unit
EGR	Exhaust Gas Recirculation
FTIR	Fourier Transform Infrared Spectroscopy
GREET	Greenhouse gases, Regulated Emissions and Energy use in Transportation
KUBI	University of Kansas Biodiesel Initiative
LCA	Life Cycle Analysis
MBT	Maximum Brake Torque
MSW	Municipal Solid Waste
NO_x	Oxides of Nitrogen
N_2O	Nitrous Oxide
PM	Particulate Matter
POME	Palm Oil Methyl Ester
PSW	Plastic Solid Waste
PtE	Pump to Exhaust
RHR	Rate of Heat Release
SO_x	Oxides of Sulfur
THC	Total Hydrocarbons
ULSD	Ultra Low Sulfur Diesel (Commercial Diesel)
VOC	Volatile Organic Compounds

WCO	Waste Cooking Oil
WLO	Waste Lubricating Oil
WPF	Waste Plastic Fuel
WtE	Well to Energy
WtP	Well to Pump
WtW	Well to Wheel

1.1 Introduction

The ever increasing energy demand along with fast depleting non-renewable fossil fuels and global climate change has led to a search for sustainable energy resources. In this area, biodiesel has shown promise through a significant amount of research. Numerous raw materials can be used to produce biodiesel that provides similar performance to that of petroleum-based diesel fuel. However, the production costs involved in the generation of biodiesel is significantly higher as compared to petroleum based fuels due to the costs involved in the fabrication of raw materials [1-3]. Thus, low cost feedstock materials for production of biodiesels have gathered significant interest among researchers across the globe.

In this thesis, the focus is on biodiesel produced from waste cooking oil (WCO) and fuel produced from plastic solid waste (PSW) since the cost of production of raw material with respect to these fuels is relatively negligible. The usage of fuels from waste not only solves environmental disposal issues but also provides an alternative sustainable energy resource. In addition, current compression ignition engines can run on diesel-like fuels with no modification to the engine architecture. However, the performance and emission characteristics of test fuels could be slightly different due to the change in their fuel properties with respect to ultra low sulfur diesel (ULSD). Thus, there is a significant need to have compression ignition engines calibrated for optimal performance of fuel while meeting modern emission regulations.

1.2 Prior and Parallel Engine Test Cell Efforts

To be able to perform a complete combustion analysis of test fuel with respect to fuel properties and knowledge of compression ignition combustion, a single cylinder test cell has been setup with a modern electronic fuel injection system, alternating current dynamometer, Fourier Transform Infrared Spectroscopy (FTIR) emission analyzer, variable sampling smoke meter, etc. in the Department of Mechanical Engineering at the University of Kansas (KU). The construction and corresponding updates of the test cell to simulate a modern commercial single cylinder compression ignition engine test have been performed by fellow Mechanical Engineering graduate students through previous efforts [4-7]. In addition, biodiesels produced from several raw materials have been prior studied in this test cell via a combustion analysis with respect to fuel properties and combustion knowledge of compression ignition engines [7-10].

The in-cylinder pressure data taken during the experimental study is fed into a thermodynamic equilibrium based heat release model developed by a fellow graduate student that is used as an extension of emission analysis of direct injected compression ignition engines [11]. This model helps to perform qualitative analysis of emission characteristics of test fuels with calculated heat release rate and in-cylinder temperatures with respect to engine crank angle degree.

1.3 Thesis Focus

This study focuses on the combustion analysis of blends of fuels produced from PSW with ULSD along with the life cycle analysis of this fuel in comparison to WCO biodiesel and ULSD. This leads into the optimization of combustion of WCO biodiesel fuel blends by employing higher fuel injection pressures to attempt to replicate the

performance of ULSD, subsequently lowering the majority of brake specific emissions of WCO biodiesel blends making it a more attractive substitute to ULSD.

Chapter 2 contains a literature review to understand the influence of synthesis technique of waste plastic fuels on its properties. In addition, a detailed review of previous efforts on combustion analysis of waste plastic fuels is provided. It is found that previous studies failed to explain performance and emission characteristics with respect to corresponding fuel properties and fuel synthesis technique. Furthermore, the combustion analysis of a commercial waste plastic fuel (WPF) blended with ULSD is accomplished and the results, both performance and emissions, are discussed with respect to changes in fuel physical properties. The outcomes suggest varying WPF influences on peak in-cylinder pressures along with premixed and diffusion burn regions as compared to ULSD. The findings suggest a fuel injection timing modification to the commercial diesel engine is required with respect to calibration for optimal performance of high waste plastic fuel blends. At lower waste plastic fuel blends, no modification to the commercial diesel engine is required without any significant changes in performance and emission characteristics.

Chapter 3 studies the life cycle analysis of waste plastic fuel and WCO biodiesel with respect to ULSD. In addition, the literature is reviewed on types of life cycle analysis performed and the tools used. It is found that majority of the studies were focused on the life cycle analysis of only the production of the fuels. In this effort, a well to exhaust (WtE) analysis is performed that consists of well-to-pump (WtP) data using the ANL GREET tool and a pump-to-exhaust (PtE) analysis using test data from the engine test cell at similar conditions. To model the synthesis technique of WCO

biodiesel, efforts of the KU biodiesel initiative (KUBI) are used, while for waste plastic fuel the literature is used to model an approximate synthesis technique. Furthermore, the WtE analysis of the test fuels are compared with that of ULSD with normalized output fuel of 36 gallons (KUBI batch capability). The WCO biodiesel is observed to have relatively lower WtP emissions for most categories; thus, this fuel is further studied in the following chapter to attempt to lower PtE emissions by employing higher injection pressures.

Chapter 4 reviews the literature regarding the influence of injection parameters on the performance and emission characteristics of ULSD, biodiesel, and WCO biodiesel fuel blends. It is observed that there is lack of studies on optimal combustion of WCO biodiesel by modulating injection parameters. Thus, this effort focuses on the influence of employing increased fuel injection pressures while normalizing injection timing for any corresponding changes in ignition delay on combustion of WCO biodiesel fuel blends. The injection pressure is increased until peak pressure of ULSD is matched at a particular load setting or no change with respect to in-cylinder pressure is seen. The results suggest that at lower fuel blends, no changes to the injection pressures are required due to negligible influence of change in fuel properties with respect to ULSD. However, at higher blends, greater fuel injection pressures are required in order to optimize the combustion performance, subsequently lowering emissions by negating the relatively high viscosity of WCO biodiesel blends. This subsequently lowers the PtE emissions and in-turn lowers corresponding WtE emissions of WCO biodiesel fuel with NO_x the only exception. Similar results could be expected for waste plastic fuel blends by employing relatively high fuel injection pressures.

Chapter 5 provides a summary of major findings of this work and helps connect outcomes of each chapter towards optimal combustion performance of waste-derived fuels. Moreover, future efforts are suggested to completely understand the outcomes of this work and move towards sustainable public transportation in around University of Kansas.

Chapter II: Combustion Analysis of Waste Plastic Fuel (Cyndiesel) Blends with ULSD

2.1 Introduction

Around the world, initiatives are being taken in order to find alternative fuels for power production to lessen global climate change. At the same time, waste plastics have created a significant environmental challenge because of their quantity and disposal issues. For example, three billion tons of waste plastic have gone to landfills in China over the last thirty years [12]. These waste plastics present in landfills produce a significant amount of methane gas contributing to climate change [13]. Since these plastics are produced from refined crude oil, they can be potentially be used to create liquid hydrocarbon fuels whose properties are close to that of existing fossil fuels. This area of waste energy recovery research includes waste cooking oil (WCO) and waste lubricating oil (WLO) in addition to waste plastics [14]. With respect to processing methods, thermal pyrolysis is one of the more promising options in order to recover the energy from this waste since only about 10% of the energy content of the waste plastic is used to create valuable hydrocarbon products and this technique is considered to be economical [14-16]. Hence, when these waste products undergo thermal pyrolysis, it yields a fuel with the highest heat of combustion value compared to other production methods [14].

2.2 Literature Review

Thermal pyrolysis is the process of thermally modifying the waste plastic (aka cracking) in the absence of oxygen subsequently converting the material into monomers, fuels, and other products [17]. The composition and quantity of liquid fuels derived from pyrolysis depends on the type of waste plastic used, temperature, and reaction conditions [15, 17-22]. Proper operation of a thermal pyrolysis reactor can yield fuels directly suited for internal combustion engine usage; e.g., fuels derived from thermal pyrolysis of waste plastic grocery bags were able to meet all ASTM D975 and EN590 fuel standards [23]. Moreover, the extent of conversion of the waste into usable engine fuels can be increased through the application of stable hydro-cracking catalysts (e.g., MgO, CaO, CdO, ZnO, Ni, and Ni-Mo) [19, 21, 24, 25]. The inclusion of a catalyst lessens the process temperature while lowering both boiling temperatures, densities of the obtained liquid products, and promotes selective degradation of waste plastics into a more useful product [19, 24]. Furthermore, studies have shown that adding iron and calcium based catalysts (e.g., Fe-C, FeOOH, and Ca-C) helps remove bromine from the liquid fuel product, subsequently decreasing the nitrogen content by converting nitrile compounds into ammonia [15]. This can reduce nitrogen oxides (NO_x) and hydrogen cyanide (HCN) emissions when this liquid fuel is used as a blend with petroleum diesel in a compression ignition (CI) engine.

While the resulting fuel product from pyrolysis is a function of waste plastic used and reactor conditions, the diesel fractions of pyrolysis oil obtained from thermal cracking of waste plastics has been observed to have a higher viscosity, density, and lower calorific value as compared to that of conventional diesel fuel [19, 20, 22, 26]. This

higher viscosity and density has been attributed to the larger aromatic content of the fuel derived through this process [27]. Furthermore, fuels derived through thermal cracking of waste plastic are said to have a lower cetane number compared to diesel. In contrast, the diesel fractions obtained through catalytic thermal cracking (e.g., kaoline, Ga-ZSM-5, and Si-Al) have been observed to have lower viscosity, density, and higher calorific value than that of diesel fuel [21, 24]. This is because these catalysts reduces the aromatic content of the fuel [17, 18, 20, 21, 24], subsequently improving the fuel qualities. This wide variance in fuel properties as a function of temperature and catalyst employed in pyrolysis indicates the variability in this field that can influence fuel economy and emissions when combusted in a CI engine.

In particular, when fuel derived from assorted waste plastics through catalytic thermal pyrolysis was used as a neat fuel, Mania et al. reported increased NO_x, carbon monoxide (CO), and hydrocarbon (HC) emissions due to a lower cetane number, reduced calorific value, and longer ignition delay in comparison to diesel. They also indicated higher brake thermal efficiencies, larger exhaust gas temperatures, and lower smoke levels for the waste plastic derived fuel. The lower smoke levels found were attributed to greater premixed combustion, faster flame propagation, and larger oxygen content in the fuel [8]. Murugana et al. also similarly found higher brake thermal efficiencies with a rise in thermal pyrolysis derived fuel (from waste tires) concentration with diesel (10%, 20%, 30%, and 50% by volume) [27]. They additionally saw greater NO_x, CO, HC, and smoke emissions that they attributed to a higher aromatic content of the derived fuel along with a longer measured ignition delay. Similar to Murugana et al., Kumar found that HC, NO_x, and CO emissions all increased with blend percentage via catalytic thermal pyrolysis

(waste high-density polyethylene, 10%, 20%, 30%, and 40% by volume with diesel) [28]. Carbon dioxide (CO_2) emissions for the blends were determined to be lower than neat petroleum diesel at almost all loads via lower brake thermal efficiencies. Whereas these researchers found significant differences during combustion when blending with waste-plastic derived fuels, Özcanli saw similar performance and emission characteristics as that of diesel fuelled engines when testing "Cyndiesel" at small quantities (5% by volume with diesel) [29]. Cyndiesel is a fuel derived from waste plastics made out of either high density polyethylene (HDPE), low density polyethylene (LDPE), polypropylene (PP), and polystyrene (PS) [30]. Finally, others have tested waste derived fuels as blends with biodiesel [31] and with the use of cooled Exhaust Gas Recirculation [32]; however, these results are not pertinent to this effort.

Of note, the absence of details of fuel synthesis technique employed in previous studies makes it difficult to attribute the appropriate reasoning of obtained performance and emission analysis towards synthesis techniques employed. However, speculating from this literature review, one may expect a fuel derived through thermal pyrolysis has a higher viscosity and density along with a lower energy content and cetane number than that of diesel. This leads to reduced atomization upon injection and an increase in fuel droplet size lowering combustion efficiency by adversely influencing the fuel and air mixing process. Moreover, one would see a longer ignition delay and an increase in fuel consumption through lower brake thermal efficiencies as combustion is delayed more into the expansion stroke. Depending on the relative magnitudes of fuel density and energy content, one might see lower or higher cylinder temperatures that would influence NO_x emissions in potentially either direction. With respect to CO and HC emissions, the

reduced mixing effectiveness and later combustion process will lead to a richer diffusion burn phase promoting incomplete combustion. Furthermore, since aromatics are a known precursor to particulate matter (PM aka smoke) emissions, one would expect to see higher PM emissions when using a waste plastic derived fuel. In the advent that a catalytic material is used in the pyrolysis process, some of these trends could be reversed as the viscosity, density, and aromatic compounds all could potentially decrease while the energy content increases.

In order to obtain a greater understanding of the effects of a waste plastic derived fuel on the CI combustion process, this effort investigates the prior mentioned Cyndiesel as a blend with common Ultra Low Sulfur Diesel (ULSD) in ratios of 5%, 10%, 20%, and 100% by volume. Cyndiesel was supplied by Cynar Plc and is derived using a proprietary catalytic thermal pyrolysis methodology using commercial and industrial packaging as the feedstock source [30]. In the following sections, the experimental setup and methodology, fuel physical properties, in-cylinder pressure traces, rate of heat release, brake specific fuel consumption, and brake specific emissions (CO, CO_2, HC, NO_x, and PM) of Cyndiesel blends are discussed in detail with respect to change in fuel physical properties from that of ULSD.

2.3 Experimental Setup

For brevity, only major instrumentation highlights will be presented here as Langness et al. [4] provides thorough documentation of the experimental setup along with the specific hardware employed. The test engine is a Yanmar L100V single cylinder direct injection CI engine with the stock mechanical fuel injection replaced with a common-rail electronic fuel injection system controlled by a Bosch MS15.1 Diesel

Electronic Control Unit (ECU). This allows for variable injection timings with resolution of 0.02 degrees per crank angle (up to five injections per thermodynamic cycle) while modulating the injection pressures 40 to 200 MPa (50.0 ± 0.5 MPa used for this study). An alternating current (AC) air-cooled regenerative dynamometer from Dyne Systems, Inc. acts to modulate the speed of the engine with load adjusted through the fuel injection amount. Torque is measured using a FUTEK transducer (Model #TRS-705) that is installed using couplings between the Yanmar engine output shaft and dynamometer input shaft. A Merriam laminar flow element (Model #50MW20-2) and an Omega differential pressure transducer (Model #PX277-30D5V) are used to measure inlet air mass flow. Fuel flow rate is characterized using a Micro-Motion Coriolis flow meter (Model #CMF010M). A Kistler (Model #6052c) pressure transducer is used to measure in-cylinder pressures and the corresponding crank angle is measured using a Kistler (Model #2614B) encoder. The stock EGR system for the Yanmar engine has been disabled, and while a cooled EGR system is available in the lab, it was not employed during the testing efforts. To characterize emissions in the exhaust stream, an AVL SESAM Fourier Transform Infrared Spectroscopy (FTIR) emission analyzer is employed. This device measures total hydrocarbons (THCs), CO, and NO_x emissions among others. Oxygen is measured using a Magnos 106 oxygen sensor. Finally, Particulate Matter (PM) emissions are monitored using AVL (Model #415S) Variable Sampling Smoke Meter.

The injection timing (standard) of the engine is calibrated for ULSD such that the minimum amount of fuel is consumed at a particular load setting. In the experimental data that follows, two sets of data are illustrated. ULSD is first tested each day to obtain reference pressure traces for a load sweep (0/25/50/75/100% of rated) ranging from 0.5

N-m to 18 N-m. Data collection occurs at a speed of 1800 RPM that represents a mid-point in the operation range of the Yanmar and because of the applicability of the results. Specifically, low-load conditions produce combustion that is primarily premixed (0.5, 4.5, and 9.0 N-m) while higher loads (13.5 and 18.0 N-m) produce combustion that is dominated by diffusion burn. Following the ULSD test, Cyndiesel blends are first tested at this standard injection timing at a particular load setting to compare its ignition delay with that of ULSD. Then, the authors normalized the injection timing of the test fuel to match the peak in-cylinder pressure trace crank angle location of ULSD at the corresponding load setting. This is done to compare the effects of fuel properties on combustion while removing the influence of ignition timing that can skew results (e.g., earlier combustion can lead to higher NO_x emissions through the thermal NO effect). The data is collected only after achieving steady-state for all the cases. Steady-state is determined based on changes in downstream exhaust gas temperatures; a change less than 1% in one minute is considered steady-state. This process is repeated for the entire load sweep. The in-cylinder pressure data taken for 60 thermodynamic cycles after steady state is reached and averaged pressure data with standard deviation is presented to analyze performance characteristics. In addition, emission data is taken for a period of five minutes after steady state is reached with one reading per second amounting to a total of 300 readings which are averaged with standard deviation is presented to analyze emission characteristics. Between tests, the fuel system is bled and flushed with the new fuel blend, subsequently running for about 30 minutes to ensure that no old fuel remains in the system. During this time, in-cylinder pressure traces are observed for changes in

ignition delay indicating combustion of the new fuel blend. Upon completion of testing, the raw data is post-processed in order to obtain averages and uncertainties.

2.4 Fuel Analysis

In order to diagnose the influence of fuel properties on combustion, the ASTM laboratory on campus was employed in order to measure the properties presented in Table 1. The specific equipment employed in determining this information includes a Koehler KV4000 Series Digital Constant Temperature Kinematic Viscosity Bath KV4000 (ASTM D445), 6200 PAAR Calorimeter (ASTM D240), Anton Paar 5000 M DMA Density meter (ASTM D4052), and Optidist distillation unit (ASTM D86). The Cetane index is obtained based on a calculated measurement based on data obtained from density and distillation tests.

Table 1. Characteristics of the fuels and blends tested.

Property	ULSD	C5	C10	C20	C50	C100
Density (kg/m^3)	841.32 ± 0.01	839.11 ± 0.01	837.00 ± 0.01	829.77 ± 0.01	818.21 ± 0.01	800.70 ± 0.01
Kinematic Viscosity (cSt)	2.74 ± 0.0044	**2.71** ± 0.0043	**2.71** ± 0.0043	**2.72** ± 0.0044	2.81 ± 0.0045	2.97 ± 0.0048
Dynamic Viscosity (cP)	2.31	2.27	2.27	2.26	2.30	2.33
Cetane Number	48.61	49.95	50.67	52.60	59.03	71.88
Energy Content (kJ/kg)	45670 ± 47	45757 ± 47	45781 ± 47	45649 ± 47	46001 ± 47	46292 ± 47
Energy Content (MJ/m^3)	38423 ± 39.96	38395 ± 39.93	38319 ± 39.85	37878 ± 39.39	37638 ± 38.76	37066 ± 38.17

The fuel injection system implemented is a high-pressure rail direct injection system that is controlled by an electronic control unit, resulting in highly accurate control of fuel injection timing and amount. It adds fuel on a volumetric basis; hence, the inclusion of the calculated MJ/m^3 row in Table 1. The ASTM laboratory data indicates

that the higher energy content and lower density of Cyndiesel leads to a relatively lower volumetric energy content in comparison to ULSD. This suggests that employing the same fuel injection pressure (as accomplished) will result in a less immediate energetic combustion event. Furthermore, the higher viscosity of Cyndiesel indicates that it is relatively more difficult to atomize the fuel leading to a reduced mixing of the fuel and air. This again suggests a lower relative release of energy from the fuel. In addition, the literature indicates a higher Cetane number for Cyndiesel [21, 24, 25, 33] (also found here), suggesting that blends and neat fuels will ignite quicker than ULSD leading to a reduced (less energetic) pre-mixed combustion phase (i.e., less fuel initially prepared). This would result in relatively lower peak in-cylinder pressures, temperatures, and oxides of nitrogen (NO_x) emissions. This leads to more fuel undergoing combustion during the diffusion burn phase and would result in relatively higher amounts of CO, THC, and particulate matter (PM) emissions. Of note, the fuel characteristics for 50% blend are shown for completeness and helps in analyzing the trends. However, this particular fuel blend was not tested due to a system malfunction and subsequent engine refurbishment after testing the other blends. Furthermore, deviations from the trends are bolded in the table and could be the result of potential operator error in running the tests.

2.5 Results and Discussion

2.5.1 In-Cylinder Pressure Traces

In Figure 1, the influence of Cyndiesel as a function of blend percentage on the in-cylinder pressure trace with respect to crank angle is presented for 0%, 50%, and 100% loads at standard (SI) and normalized (NI) injection timings close to top dead center (TDC). On comparison, the in-cylinder pressures at standard injections suggest an

earlier in-cylinder pressure rise with an increase in Cyndiesel percentage indicating quicker combustion. This insinuates a shorter ignition delay as compared to that of ULSD and a relatively higher Cetane number for Cyndiesel blends as previously found in the literature and proven through fuel characteristics shown in Table 1.

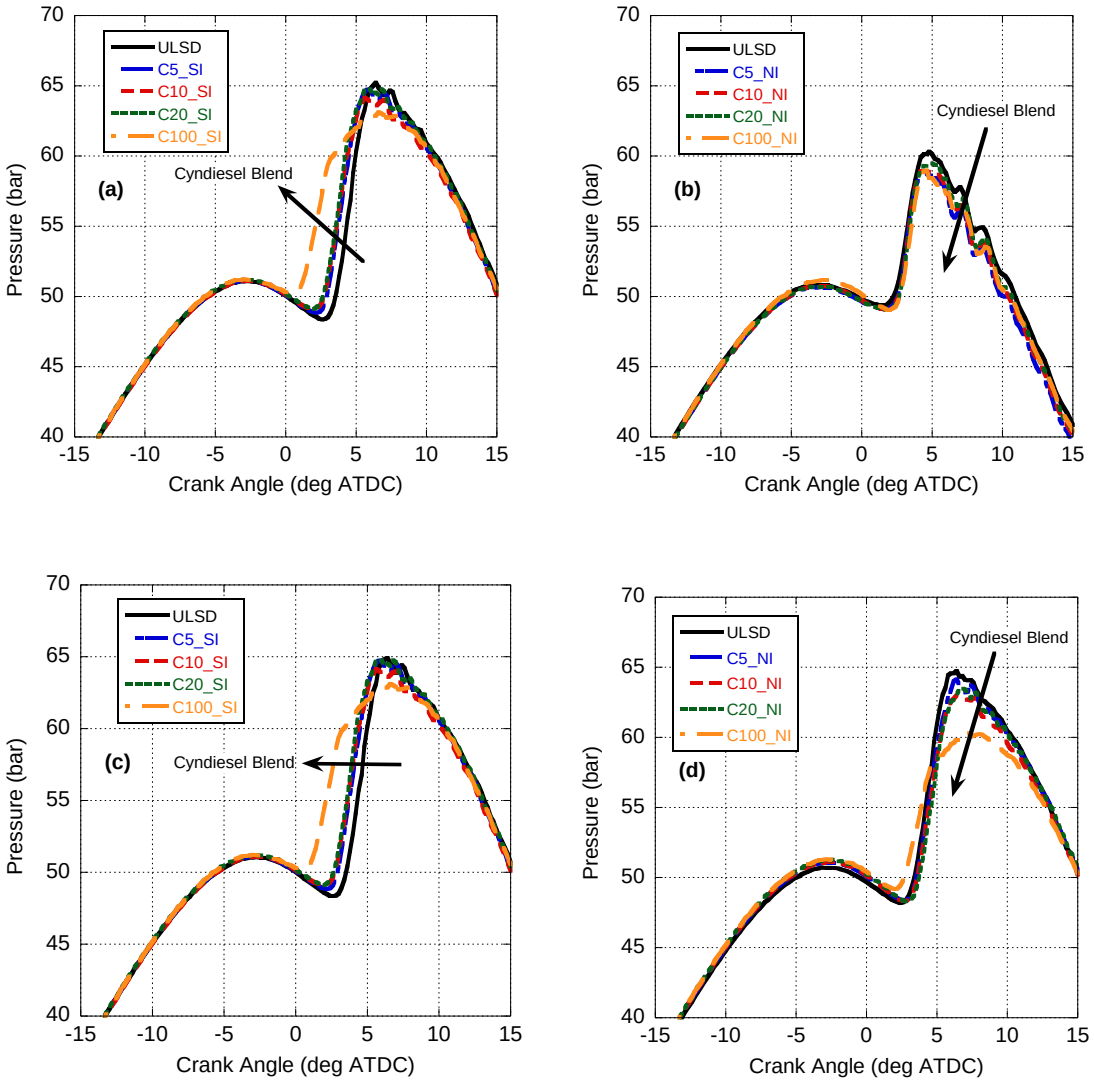

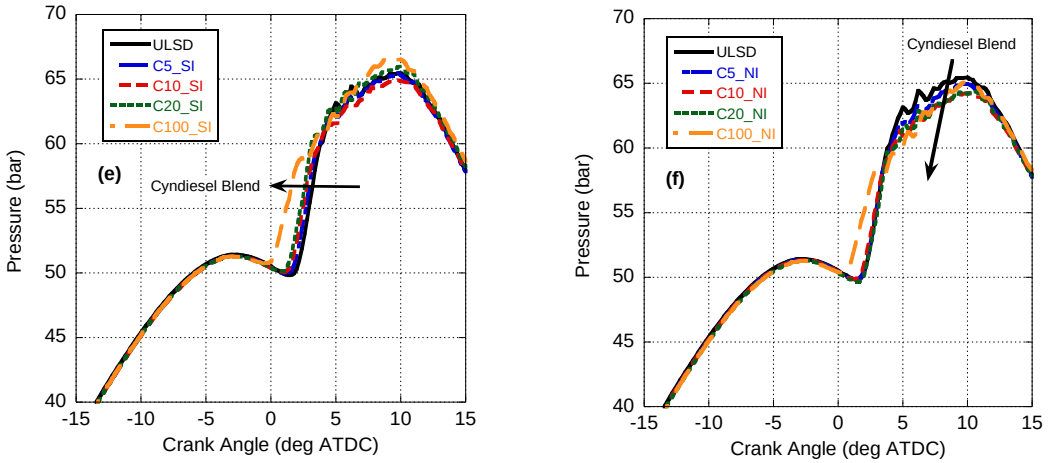

Figure 1. In-cylinder pressure traces with respect to crank angle for 0% (a, b), 50% (c, d), and 100% (e, f) load as a function of Cyndiesel volume percentage at standard (a, c, e) and normalized (b, d, f) injection timing

As mentioned prior, the injection timings of Cyndiesel blends were then normalized to match the crank angle location of the peak in-cylinder pressure of ULSD at corresponding loads. Thus, effects of combustion phasing due to changes in ignition delay on performance and engine emissions are removed. ULSD is observed to have the highest peak in-cylinder pressures at all load conditions. At 0% load, the in-cylinder pressure traces of Cyndiesel blends are not too dissimilar from that of ULSD. This is due to lower amounts of fuel being combusted and, thus, a smaller influence of change due to fuel physical properties. As the load increases, noticeable drops in peak in-cylinder pressures are observed with greater percentages of Cyndiesel in the blend due to a larger influence of fuel properties. As previously discussed, fuel is injected on volumetric basis and the lower energy per unit volume of Cyndiesel suggests a reduced pre-mixed burn and lower peak in-cylinder pressures. Furthermore, the relatively higher viscosity of Cyndiesel indicates that it is more difficult to atomize. This leads to larger fuel droplets and affects mixture preparation negatively resulting in another factor lowering the pre-

mixed burn phase and peak in-cylinder pressures. Finally, the higher Cetane number of the Cyndiesel leads to a shorter ignition delay and relatively less amount of fuel available for the premixed phase of combustion. These all collectively promote lower peak in-cylinder pressures and reduce the pre-mixed burn phase with an increase in percentage of Cyndiesel in blend and load.

2.5.2 Rate of Heat Release

Computing the heat release rate of the fuel blends helps to further illustrate the influence of Cyndiesel fuel properties upon combustion. The rate of heat release at each crank angle is calculated in Figure 2 using a model based on a chemical equilibrium estimation of cylinder contents satisfying the first law of thermodynamics [10]. The shift in heat release of Cyndiesel blends away from TDC relative to ULSD at standard injection timing, which becomes more pronounced with Cyndiesel percentage, again suggests earlier combustion and is due to the higher Cetane number for Cyndiesel.

On normalizing the injection timing, at 0% load the peak rate of heat release is similar across the Cyndiesel blends and ULSD. However, as load increases, an observed drop is seen in the peak rate of heat release for Cyndiesel blends relative to ULSD. This reduction in the pre-mixed burn phase leads to a corresponding increase in diffusion burn phase (most notable beyond the 50% load setting). As mentioned in regards to the in-cylinder pressure trace discussion, the relatively higher viscosity, lower volumetric energy content, and greater Cetane number of the Cyndiesel leads to a shorter ignition delay and relatively less amount of fuel available for the premixed phase of combustion (and subsequent increase in diffusion burn).

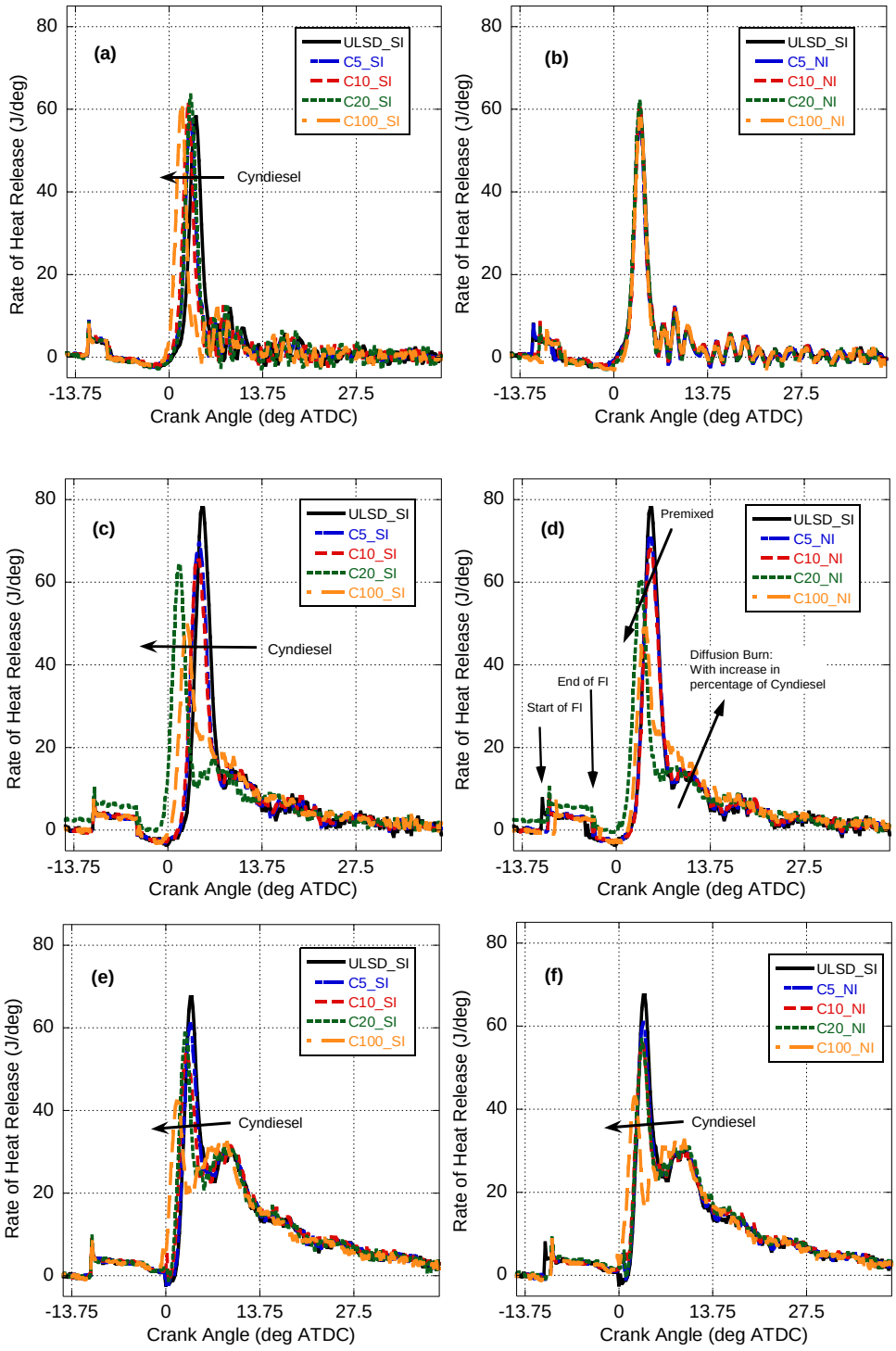

Figure 2. Heat release rates with respect to crank angle for 0% (a, b), 50% (c, d), and 100% (e, f) load as a function of Cyndiesel volume percentage at standard (a, c, e) and normalized (b, d, f) injection timing

2.5.3 Brake Specific Fuel Consumption

Of note, the rate of heat release during the fuel injection period is positive in Figure 2 as opposed to negative due to the loss of heat from cylinder gases due to fuel vaporization. This anomaly is due to an assumption in the heat release model that injected fuel is instantaneously atomized and vaporized; thus, adding energy to the gas from the liquid fuel immediately. This was done to reduce the computational effort involved in developing the model. While erroneous, this is helpful in the diagnosis of the brake specific fuel consumption trends in Figure 3. In specific, the overall length of injection between ULSD and Cyndiesel blends does not differ noticeably and brake specific fuel consumption values are similar with no observable trends with Cyndiesel blend. This is because the energy content per mass of Cyndiesel is higher, resulting in the need for less total mass in order to achieve the same torque. In other words, the reduction in constant volume combustion and thermal efficiency through a lower volumetric energy content of Cyndiesel is overcome via a higher mass-based energy rich fuel.

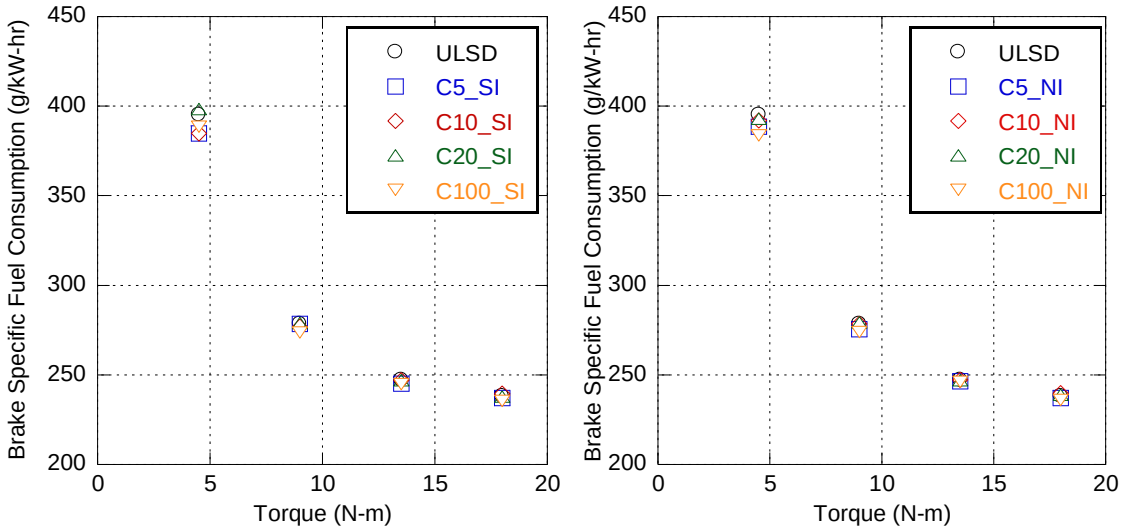

Figure 3. Brake specific fuel consumption vs. engine torque for standard and normalized injection timing (note: error bars are not included)

2.5.4 In-Cylinder Temperature Traces

To investigate the combustion process further, in-cylinder temperature is employed as calculated from the measured pressure data via the heat release model. As shown in Figure 4, the results with standard injection timing suggest earlier combustion with a faster rise in temperatures due to higher Cetane number of Cyndiesel as compared to ULSD. For the normalized injection comparisons, since combustion phasing is adjusted by peak pressure location, the peak temperatures do not necessarily align. Moreover, the initial temperature before combustion begins (i.e., compression temperatures) may differ due to the relative amount of heat transfer and exhaust gas temperatures. For instance, a hotter in-cylinder combustion process will promote more heat transfer to the walls raising the gas temperature during the following compression process. Furthermore, a hotter exhaust gas will result in a warmer in-cylinder residual, increasing the initial charge temperature. This is evident in Figure 4(i) for the high Cyndiesel percentages; peak temperature is higher resulting in a hotter compression temperature.

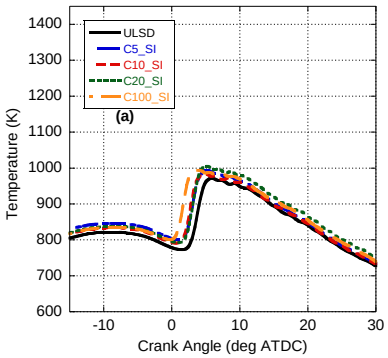
ULSD
C5_SI
C10_SI
C20_SI
C100_SI
(a)
Temperature (K)
Crank Angle (deg ATDC)

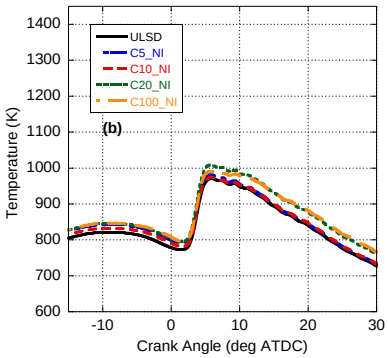
ULSD
C5_NI
C10_NI
C20_NI
C100_NI
(b)
Temperature (K)
Crank Angle (deg ATDC)

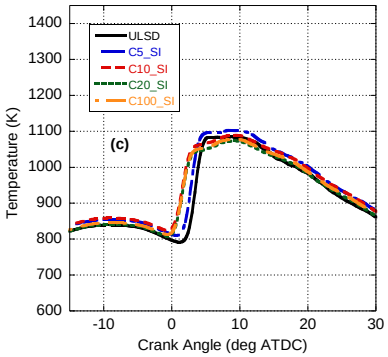
ULSD
C5_SI
C10_SI
C20_SI
C100_SI
(c)
Temperature (K)
Crank Angle (deg ATDC)

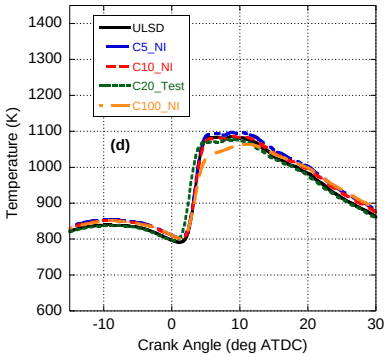
ULSD
C5_NI
C10_NI
C20_Test
C100_NI
(d)
Temperature (K)
Crank Angle (deg ATDC)

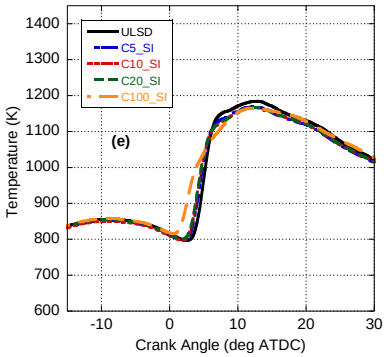
ULSD
C5_SI
C10_SI
C20_SI
C100_SI
(e)
Temperature (K)
Crank Angle (deg ATDC)

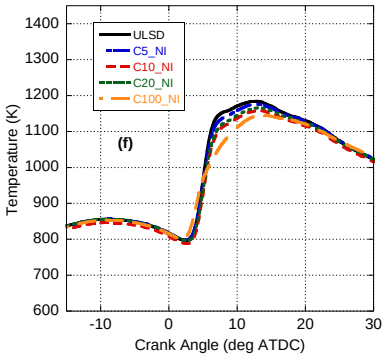
ULSD
C5_NI
C10_NI
C20_NI
C100_NI
(f)
Temperature (K)
Crank Angle (deg ATDC)

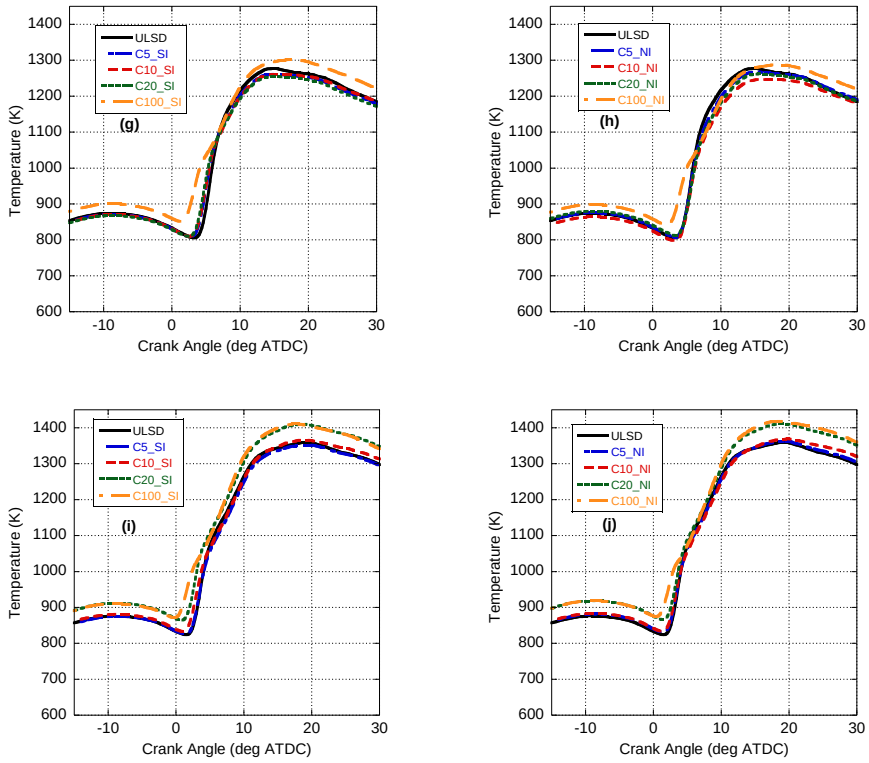

Figure 4. Cylinder temperature vs. engine crank angle at 0.5 N-m (a, b), 4.5 N-m (c, d) 9.0 N-m (e, f), 13.5 N-m (g, h), and 18.0 N-m (i, j) at standard (a, c, e, g, i) and normalized (b, d, f, h, j) injection timings

Before discussing the temperature trends, three previous items are summarized:

1. Between 0.5 and 9.0 N-m, combustion is primarily pre-mixed (see Figure 2(a) through Figure 2(d)).
2. As more Cyndiesel is added, the pre-mixed spike continually decreases due to inherent fuel properties.
3. The brake specific fuel consumption values are nearly equivalent (within experimental error) indicating that the same amount of fuel is added between ULSD and Cyndiesel blends (resulting in a greater potential energy release as Cyndiesel percentage increases).

From this information, it is anticipated that the maximum temperature between 0.5 and 9.0 N-m should go down with added Cyndiesel. The reduced amount of pre-mixed combustion leads to less constant volume combustion and a subsequent slower (and colder) burn. This is largely what is seen in the data via Figure 4 with a few outliers. However, above 9.0 N-m, the temperature generally increases with Cyndiesel blend. This is presumed due to item #3 in the summary as more energy is released during the combustion event. This is buffered somewhat due to a poorer mixing and combustion process due to a higher viscosity; e.g., the trend at 13.5 N-m is not well defined. Now, while it is true that item #3 still plays a role between 0.5 and 9.0 N-m, there is significantly less fuel combusted; hence, item #2 has a larger influence.

2.5.5 Brake Specific Emissions

The performance analysis is used in conjunction with fuel physical properties to analyze brake specific emissions at all loads and injection strategies. Emissions presented as a function of engine brake torque are called brake specific emissions. The brake specific emissions of oxides of nitrogen (NO_x), carbon monoxide (CO), total hydrocarbons (THC), and particulate matter (PM) are shown as a function of engine brake torque with comparisons between standard and normalized injection timings in the following sections. There is observed a higher variability at 0.5 N-m loading due to significance of torque spikes at this load because of the single cylinder engine design.

2.5.5.1 Brake Specific NO_x Emissions

The brake specific NO_x emission results in Figure 5 are composed of a collection of nitric oxide (NO) and nitrogen dioxide (NO_2). These NO_x compounds are typically formed in lean and high temperature zones of combustion. The relatively lower pre-

mixed burn regions for Cyndiesel blends are observed as the percentage of Cyndiesel in the blend increases in Figure 3. This indicates relatively colder burn (i.e., less constant-volume combustion) and subsequently lowers in-cylinder temperatures during this phase for Cyndiesel blends compared to ULSD as illustrated in Figure 4. Since the majority of combustion event between 0.5 N-m and 9.0 N-m is premixed, this leads to lower amounts of brake specific NO_x emissions for Cyndiesel blends as shown in Figure 5(b) for these loads. As the load increases beyond 9.0 N-m until 18.0 N-m, relatively higher amounts of diffusion burn regions are observed for Cyndiesel blends as shown in Figure 3. This leads to a relative increase in in-cylinder temperatures for Cyndiesel blends during the latter part of combustion as shown in Figure 4. In addition, at full load the engine operates at a global equivalence ratio of 0.75 around the ideal conditions of temperature and oxygen for NO_x formation. This results in an increase of late NO_x formation, while the relative decrease in premixed burn for Cyndiesel blends at these loads leads to reduced initial NO_x formation. The net effect for mid to high-loads in Figure 5(b) is that while NO_x emissions do decrease with Cyndiesel percentage due to a lower pre-mixed burn and less initial NO_x formation, the added energy during the diffusion burn phase results in enhanced late NO_x formation pushing the Cyndiesel results closer to ULSD. Investigations on the influence of combustion phasing on brake specific NO_x emissions are inconclusive within experimental error, as shown in Figure 5(a) and 5(b). However, the early combustion of Cyndiesel blends due to a higher Cetane number is expected to increase early NO_x formation and, thus, lead to increased brake specific NO_x emissions compared to the case with normalized injection timing.

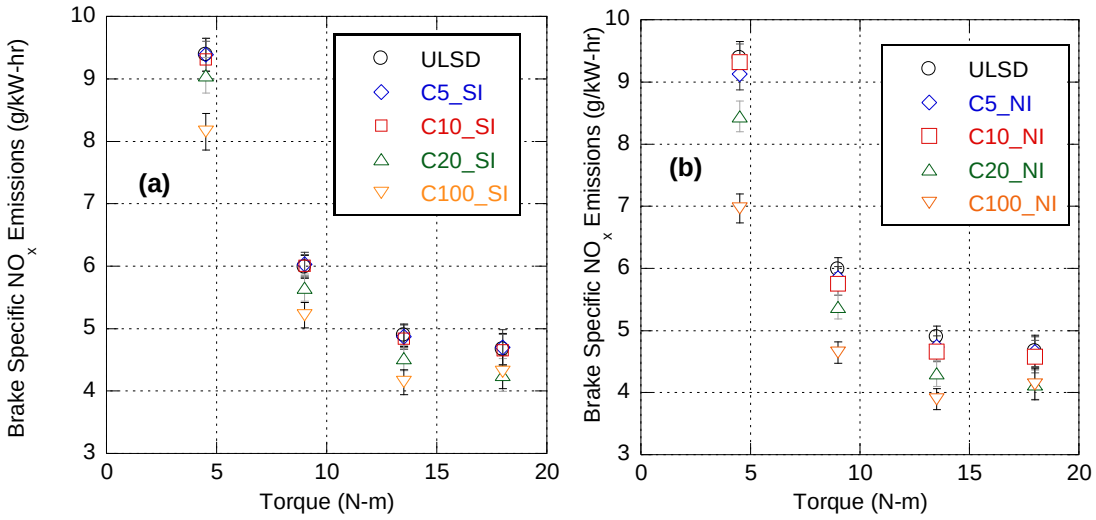

Figure 5. Brake specific NO_x emissions vs. engine torque for (a) standard and (b) normalized injection timings

2.5.5.2 Brake Specific CO and THC Emissions

The brake specific CO and HC emissions are shown in Figure 6 and Figure 7 with increasing load, respectively. These emissions are formed primarily due to inefficient combustion with the dissociation of CO_2 at high temperatures providing another potential factor for CO production. Between 0.5 N-m and 9.0 N-m loading, the Cyndiesel blends have relatively lower combustion efficiencies due to poorer atomization and vaporization as compared to ULSD. This leads to the anticipation of higher brake specific CO and HC emissions at these loads. However, with respect to CO, the lower premixed burn regions for Cyndiesel blends results in lower in-cylinder temperatures that reduce CO_2 dissociation levels. This offsets the expected result slightly; however, the combustion efficiency effect is assumed to dominate. Above 9.0 N-m loading, the combustion efficiency continues to degrade for Cyndiesel blends due to significantly higher diffusion (rich-) burn regions. However, (for the most part) higher in-cylinder temperatures are seen that would increase combustion efficiency and reduce CO and HC emissions, while

additionally promoting some CO_2 dissociation. Overall, at higher loads, the significant increase in rich-burn combustion is assumed to dominate and brake specific CO and HC emissions for Cyndiesel blends are anticipated to be higher as compared to ULSD. However, the experimental results indicate opposite trends at all of the loads tested.

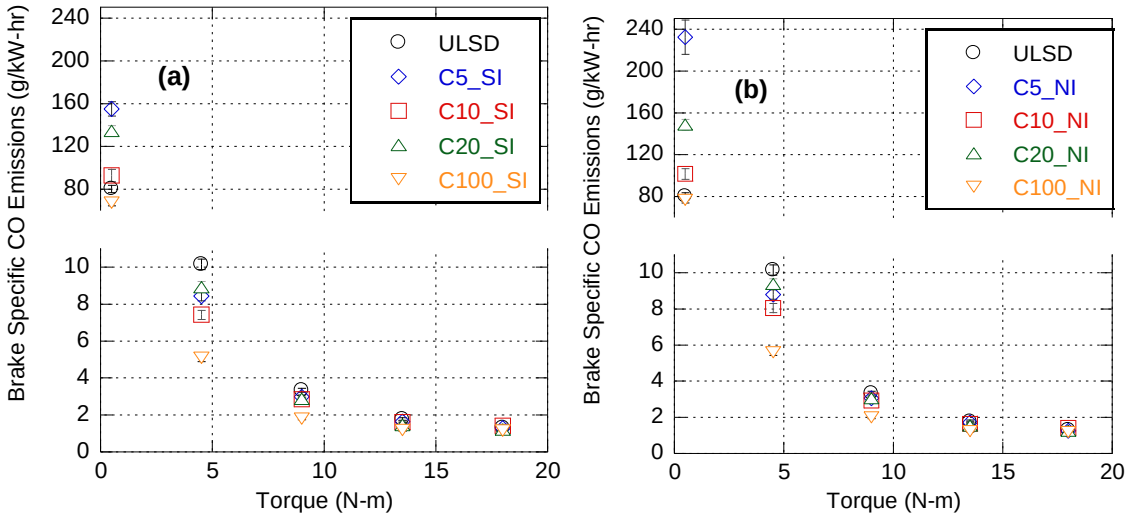

Figure 6. Brake specific CO emissions vs. engine torque for (a) standard and (b) normalized injection timings

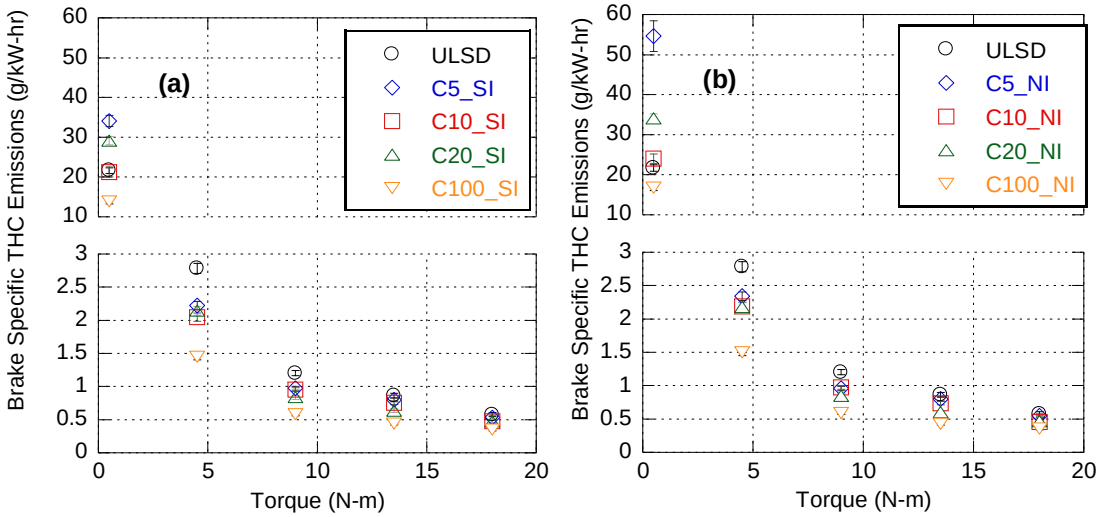

Figure 7. Brake specific THC emissions vs. engine torque for (a) standard and (b) normalized injection timings

As a result, it is believed that the unknown chemistry of fuel is playing a significant role in CO and HC formation. Thus, in an attempt to understand the composition of fuel and fuel chemistry, It is believed from the literature that H:C ratios probably do change since aromatics are in general are considered to be lower with respect to feedstock material as compared to that of ULSD.

The literature suggests that employing a catalytic pyrolysis synthesis results in the reduction of unsaturated bonds and a subsequent increase in saturated bonds in the fuel product [21, 24, 25]. Since the fuel synthesis technique employed in production of Cyndiesel is a proprietary catalytic pyrolysis, this literature finding partially explains reversion of CO and HC trends. In specific, it is theorized that Cyndiesel has a larger percentage of C-H bonds (i.e., saturated) than C═C bonds (unsaturated). Hence, adding Cyndiesel to ULSD possibly reduces the number of stronger double bonds with weaker hydrogen-carbon bonds making the fuel blend relatively easier to combust. As a result, this would lead to the reduction in CO and THC emissions with Cyndiesel percentage as found.

On comparing trends between standard and normalized injection timings, within experimental error there is no well-defined trend within the data. In theory, normalizing the timing for the higher Cetane number of Cyndiesel would result in a greater (richer) diffusion burn phase and higher CO and HC emissions.

2.5.5.3 Brake Specific PM Emissions

Particulate Matter (PM) emissions are typically formed when combustion happens around a fuel rich core. The Cyndiesel blends are generally observed to have higher amounts of brake specific PM emissions as shown in Figure 8 over the entire load range.

This is primarily due to poorer atomization of this fuel based on its relatively higher viscosity. This leads to lower amounts of premixed burn and higher amounts of diffusion burn as the percentage of load increases as shown in Figure 2. However, at full load, the brake specific PM emissions for higher Cyndiesel blends fall below lower Cyndiesel blends due to the postulated decrease in unsaturated bonds. Of note, aromatic (unsaturation) compounds in fuel blends are a precursor for formation of PM emissions. Hence, at high Cyndiesel fuel blends, enough unsaturated species and aromatic compounds in ULSD may have been replaced with saturated species to cause a reduction in PM emissions. Furthermore, higher in-cylinder temperatures are observed at higher blends in Figure 4(j) because of the higher mass-based energy content of Cyndiesel at full load. This improves fuel vaporization and mixture preparation despite poorer atomization. This would further reduce high blend PM emissions in comparison to lower blends. Finally, the brake specific PM emissions between standard and normalized injections are observed to be comparable. Similar to CO and HC, one would expect higher PM emissions when adjusting injection timing for a greater Cetane number; i.e., later injection timing and greater level of diffusion burn.

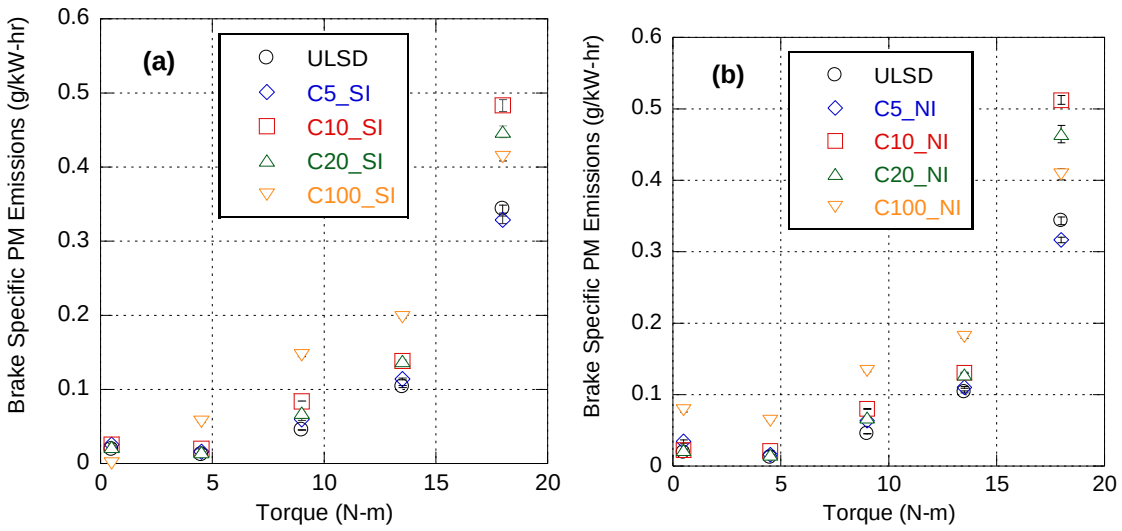

Figure 8. Brake specific PM emissions vs. engine torque for (a) standard and (b) normalized injection timings.

2.6 Conclusion

The current industry focus on alternative fuels is a result of increasing energy demands while considering a finite quantity of fossil fuels. In this area, waste plastics could potentially act as a relatively abundant source of alternative fuels. Any fuel derived from waste plastics is certainly different from commercial diesel with respect to its physical properties. As a result, it is necessary to understand the combustion of these fuels in compression ignition engines in order to optimize fuel performance while maintaining emission standards.

This study blended a commercial waste plastic fuel (Cyndiesel) derived from plastic solid waste with ULSD for testing within a single-cylinder compression ignition engine that employs a modern fuel injection system. All Cyndiesel blend properties were found using an ASTM laboratory on campus and compared to that of neat ULSD. With respect to increasing Cyndiesel blend percentage, density is observed to decrease while

viscosity and energy content by mass increased (it did decrease by volume). Combustion analysis was subsequently performed for each fuel blend at five load cases ranging between (0.5 N-m to 18.0 N-m) at consistent load settings. Peak pressure decreased while the rate of diffusion burn increased with growing Cyndiesel blend percentage. Largely because energy content by mass increased, there was no noticeable difference in fuel consumption and temperatures within the cylinder were relatively similar or greater with increasing blend percentage at the highest loads.

However, even though temperatures were equal to or greater than ULSD, it was generally found that brake specific NO_x emissions decreased with Cyndiesel blend percentage due to a reduction of the pre-mixed burn phase. Furthermore, brake specific PM emissions increased with blend and then decreased while CO and THC emissions were reduced. The lower brake specific CO and THC emissions and lower PM emissions at high blend percentages are observed to contradict with the anticipated results based on compression ignition combustion behaviour and fuel viscosity. This could be due to a relative replacement of unsaturated bonds with saturated bonds as Cyndiesel percentage increased making the fuel relatively easier to combust. It is believed that further investigation into the fuel chemistry could help explain the seemingly contradictory trends. Moreover, future efforts should employ a higher fuel injection pressure in order to improve the atomization of Cyndiesel blends due to its higher viscosity than ULSD. This could help mitigate the increased PM emissions while still achieving NO_x emissions below that of neat ULSD. Finally, a complete feedstock to tailpipe analysis of the conversion of waste plastics against other potential waste feedstocks (e.g., waste cooking

oil biodiesel) should be accomplished in order to frame the findings in the appropriate comparative light.

Chapter III: Life Cycle Analysis of Waste Cooking Oil Biodiesel, Waste Plastic Fuel, and ULSD from Well to Exhaust

3.1 Introduction

The previous chapter analyzed the combustion and emission characteristics of a fuel derived from waste plastics (WPF). While the results appear promising, it is important to understand the big picture of waste-derived fuels in comparison to that of traditional fossil fuels, such as Ultra Low Sulfur Diesel (ULSD). In order to accomplish this, a full Life Cycle Assessment (LCA) must be done in order to compare the energy used and emissions generated from Well-to-Wheels (WtW). Since WPF, Waste Cooking Oil (WCO) biodiesel, and ULSD have been tested at the University of Kansas (KU) using the same engine running at similar conditions (e.g., speed, fuel injection pressure, etc.), this effort will compare these fuels using a full Well-to-Exhaust (WtE) analysis providing normalized results on a $g_{emissions}/kg_{fuel}$ basis. This will help researchers understand the benefits (or drawbacks) of using waste products as a feedstock in the transportation environment. As the control volume for analysis, the University of Kansas (KU), Lawrence campus is chosen since the quantities of WCO and waste plastic collected are known through the KU Biodiesel Initiative (KUBI) and KU Recycling efforts, respectively. In addition, the KUBI currently processes WCO into biodiesel and further research is underway on waste plastic fuel synthesis in an attempt to move towards sustainable fuel production for on-campus public transportation.

In this chapter, the WtE analysis is performed with the help of the Greenhouse gases, Regulated Emissions, and Energy use in Transportation (GREET) model (version

GREET.net 2014) developed by Argonne National Laboratory [34]. This model employs a database to compare the hazardous and greenhouse gas (GHG) emissions and energy consumed during successive processes involved in production, logistics, and usage of transportation fuels.

The GREET model estimates the amount of emissions produced and energy consumed based on upstream conditions, defined energy inputs, and their respective sources when stationary. When transporting fuels, the mode of transportation, distance covered, resource transported, and payload are defined to enable the model to estimate energy emissions generated during this process. In addition, the GREET model cumulates all the emissions produced and energy used at the end of production pathway [35]. However, prior to performing said effort, it is important to review the LCA literature in this area with respect to WCO biodiesel and WPF.

3.2 LCA Literature Review for Waste Cooking Oil Biodiesel

Since WCO is considered a waste with no requirement of additional energy and material for its formation, researchers have indicated that there is not any environmental impact in its formation [30, 36, 37]. Tu and McAvoy highlight this in a pilot study through employing an LCA of a centralized plant at University of Cincinnati to produce biodiesel from WCO illustrating the elimination of transportation for its disposal. Moreover, their findings indicate that the conversion of WCO to biodiesel on campus saw an approximate reduction of 9.37 tonnes of carbon dioxide (CO_2) eq/yr [38]. This finding is corroborated in work by Iglesias et al. who mention that a centralized production methodology is significantly better for production facilities relatively small in size (e.g., a college campus) since transportation of the source feedstock is minimized [37].

With respect to conversion of WCO to a biodiesel fuel, there have been several LCA studies performed. For instance, Varanda and Martins used four categories of damage (i.e., human health, ecosystem quality, climate change, and resources) to analyze the environmental influence of biodiesel produced from palm oil and waste cooking oil using the Ecoinvent database and IMPACT 2002 tool [39]. The results of this study suggest that the LCA of biodiesel produced from WCO has a lower environmental impact as compared to virgin oils. Moreover, the synthesis of WCO biodiesel via alkaline catalysis with acid pretreatment to remove free fatty acids (FFA) is observed to have the lowest impacts on human health and ecosystem quality than other the production alternatives studied (acid catalysis and supercritical methanol process) using WCO and virgin oils. Of note, the KUBI process employs the alkaline catalyzed process with potassium hydroxide as the catalyst.

Similarly, Morais et al. categorized potential environmental impacts, such as abiotic resource depletion and ozone layer depletion, when performing the LCA of biodiesel produced from WCO using three different transesterification processes: alkali catalyzed, acid catalyzed, and supercritical methanol [36]. The results of this study suggest differently than Varanda and Martins that the most environmentally favorable alternative is the supercritical methanol process with propane as a co-solvent followed by the alkaline catalyzed process with acid pretreatment of FFAs and subsequently the acid catalyzed process. This is because propane used as co-solvent in this supercritical methanol process decreases the oil to alcohol molar ratio along with the reaction temperatures and pressures required while the catalyzed transesterification processes use more chemicals, expensive catalysts that get poisoned over time, and significant amounts

of water [40]. In addition, the acid catalyzed process uses greater amounts of methanol than the alkaline catalyzed process subsequently making this process the most environmentally unfavorable as compared to other alternatives [36]. However, with respect to the supercritical methanol process, Kiwjaroun et al. determined that while this is a simple production process with relatively low reaction times, higher yields, and lower production of environmentally damaging wastes, it requires significant amounts of methanol. This results in a greater influence on the environment than conventional processes because it uses higher amounts of methanol along with greater reaction temperatures and pressures without an appropriate co-solvent. Hence, this process is energy intensive in the production of biodiesel fuels and recycling of methanol [41]. Therefore, with respect to the KUBI conversion process, it appears it has the lowest environmental influence of the biodiesel production processes. With respect to this transesterification process, Peiro et al. found that it accounts for about 68% of WCO's environmental impact as categorized similarly to Morais et al. [30]. Furthermore, Pleanjai and Garivait indicate that GHG emissions from the WCO biodiesel transesterification production pathway are 93% less than that of conventional diesel production [42].

Additional research in this area finds a study performed on six different biodiesel pathways in China by Xunmina et al. uses a custom model (Tsighua-CA3EM) to include the dominance of coal usage for supplying production energy (similar to Lawrence, KS) along with using transportation energy requirements from the GREET model [43]. The results suggest that the biodiesel fuels produced from jatropha and WCO employing cassava-derived ethanol in the transesterification process can reduce both fossil fuel consumption and GHG emissions as compared to the conventional diesel pathway.

However, employing corn derived ethanol and soybean biodiesel can only reduce fossil fuel consumption in comparison to diesel. Moreover, using a sorghum derived ethanol pathway increases both fossil fuel consumption and GHG emissions relative to diesel.

Finally, separate from the more traditional biodiesel production processes, using an LCA study Yanoa et al. suggest that hydrogenation (i.e., thermally cracking WCO at 400-500°C followed by distillation to separate the fuel and then refining to remove the acid prior to hydrogenation using H_2 at 150-250°C) would be more attractive than transesterification processes to meet long term Japanese emission standards [44]. This is because hydrogenation improves the stability of refined biodiesel for oxidation and heat, promoting better fuel storage characteristics while additionally having a lower environmental impact than transesterification. Moreover, Mendoza et al. suggest that a multi-objective production methodology could have a slight environmental gain over the single objective production methodology [45]. This is because in the multi-objective concept the byproducts are used for alternate product lines and the remaining residue is recycled to be used in the next batch; whereas, the single objective idea is to obtain only the main product. Therefore, with respect to an LCA, the multi-objective production methodology has proven to have a lower environmental impact. This multi-objective concept is the basis for other efforts at KU involving glycerin (a by-product of biodiesel production through the transesterification process) conversion to a syngas for power production [46]; however, incorporating these findings are beyond the scope of this current LCA. Of note, glycerin in this effort is considered a valuable product (e.g., used in the food industry) and is not subject to disposal or further LCA analysis.

3.3 LCA Literature Review for Waste Plastic Fuels

There are several challenges involved in utilizing the energy potential of waste to reduce dependency on non-renewable fossil fuels while minimizing environmental impact. Land filling is the traditional technique employed for waste disposal; this leads to unpredictable emissions and contaminates air and water, causes irreversible damage to soil, and occupies large amounts of land [16, 47, 48]. Because of these issues, a conventional thermal treatment technique called incineration is being employed for waste management to lower the usage of landfills. Besides waste disposal, incineration generates electricity but uses fossil fuels for auxiliary heating, contributes to CO_2 emissions, and contains toxic contaminants [16, 49, 50]. In comparison to incineration, several LCA studies have shown that modern thermal treatment techniques like pyrolysis, gasification, co-combustion, co-utilization, and co-processing via an integrated approach possess improved waste utilization, combustion efficiency, and energy efficiency while having a significantly lower environmental influence [47, 49-52]. In this area of study, pyrolysis of Municipal Solid Waste (MSW) or Plastic Solid Waste (PSW) is attractive to reduce emissions because it retains the sulfur, chlorine, alkali, and heavy metals within the solid residues while reducing thermal nitrogen oxides (NO_x) formation due to lower operating temperatures and reducing conditions (i.e., rich combustion) as compared to incineration [51]. Thermal pyrolysis and catalytic pyrolysis are the two types of techniques employed in pilot plants to derive liquid fuels close to that of conventional diesel and gasoline in chemical structure by breaking down complex polymers in the absence of oxygen.

With respect to this effort, non-availability of the sensitive technological details for catalytic pyrolysis of the WPF (Cyndiesel) used in previous chapter led to further research in order to approximate a thermal pyrolysis process and perform a representative LCA. In general, catalytic pyrolysis is relatively more complex to analyze because the performance of this process is a function of several parameters like type of catalyst, size of catalyst particles, physical structure, necessary pretreatment of catalyst, and several other reaction conditions. Of note, this process often uses lower operating temperatures while resulting in higher yields and products that are of shorter carbon chain length (C_1 to C_{11}), making them more similar in structure to transportation fuels; however, this results in higher operating costs [21, 53, 54]. In addition, the catalyst involved deactivates over time and it has to be regenerated for consistency in product yield. Thus, approximation of such a highly nonlinear process would result in an inaccurate model for a WtE analysis. Therefore, a representative thermal pyrolysis process will be employed because of its relative simplicity. As a result, the outcomes of the LCA must be considered approximate at best.

The experimental setup chosen for thermal pyrolysis is a packed bed reactor with cement powder as the bed material. Shredded, cleaned, and dried PSW (coming from KU Recycling) acts as the feedstock and nitrogen is used to purge the reactor to maintain an inert environment. The reactor is heated at the rate of 15 °C/min and maintained at 500 °C and atmospheric pressure for 45 minutes. This information was translated to a GREET specific model as described in the WPF section. The pyrolysis gases are passed through a cooling coil and to a condensation tank where the liquid is collected. The literature suggests that the liquid (i.e., WPF) yield would be about 80-82% by mass, and the gas

emissions would be about 18-20% [16, 51, 53-55]. For simplicity in the LCA comparison, any solid residues remaining from the WCO biodiesel and thermal pyrolysis production processes are considered negligible in mass with respect to the end products of biodiesel, glycerin, WPF, and gas emissions.

3.4 LCA Concept Employed

Most of the LCA studies available in the literature are based on either a Well-to-Pump (WtP) or WtW analysis. However, available data from a WtW analysis employs information generated by a wide number of researchers using different engines and, potentially, dissimilar testing methodologies. Hence, this information could provide a skewed viewpoint of the energy and emissions of WCO biodiesel versus WPF and conventional diesel. Moreover, this prior information does not necessarily provide researchers with a direct answer as to what engine parameters should be modulated to improve combustion for lower emissions. As a result, this WtE study includes a summation of a WtP analysis performed using the GREET model and PtE combustion analyses of the respective fuels in a single cylinder compression ignition (CI) engine test cell at similar conditions (i.e., same injection pressures, equivalent peak pressure crank angle location with ULSD at each engine load, etc.). Hence, a truer LCA representation of each fuel is achieved in this work. With respect to the literature findings, one would expect lower GHG emissions and energy consumed for production of WCO biodiesel as compared to ULSD. Similar studies performed at the University of Cincinnati with an on-site pilot plant to produce WCO biodiesel via the alkaline transesterification process with sodium hydroxide as catalyst shows 50% lower GHG emissions and has the potential to replace 19% of the diesel consumed over the LCA [38]. With respect to WPFs, the author

is unable to find any information in the literature comparing an LCA with ULSD. Hence, this work will add to the literature by documenting the LCA of a WPF while additionally comparing its outcomes to ULSD and another waste derived fuel (i.e., WCO biodiesel).

3.5 WtE Analysis of WCO Biodiesel

The WtE analysis of WCO biodiesel includes the summation of well to pump (i.e., production and transportation of the fuel) and pump to exhaust (i.e., combustion) analysis performed separately in the author's laboratory. This combustion analysis will be described in depth in the following chapter (i.e., the standard injection findings are used here). The well to pump analysis of WCO biodiesel consists of the following processes:

- Storage of WCO
- Collection of WCO
- Filtration & Thermal Treatment of WCO
- WCO Biodiesel Synthesis
- Washing of WCO Biodiesel
- Thermal Drying of WCO Biodiesel
- Transportation of WCO Biodiesel

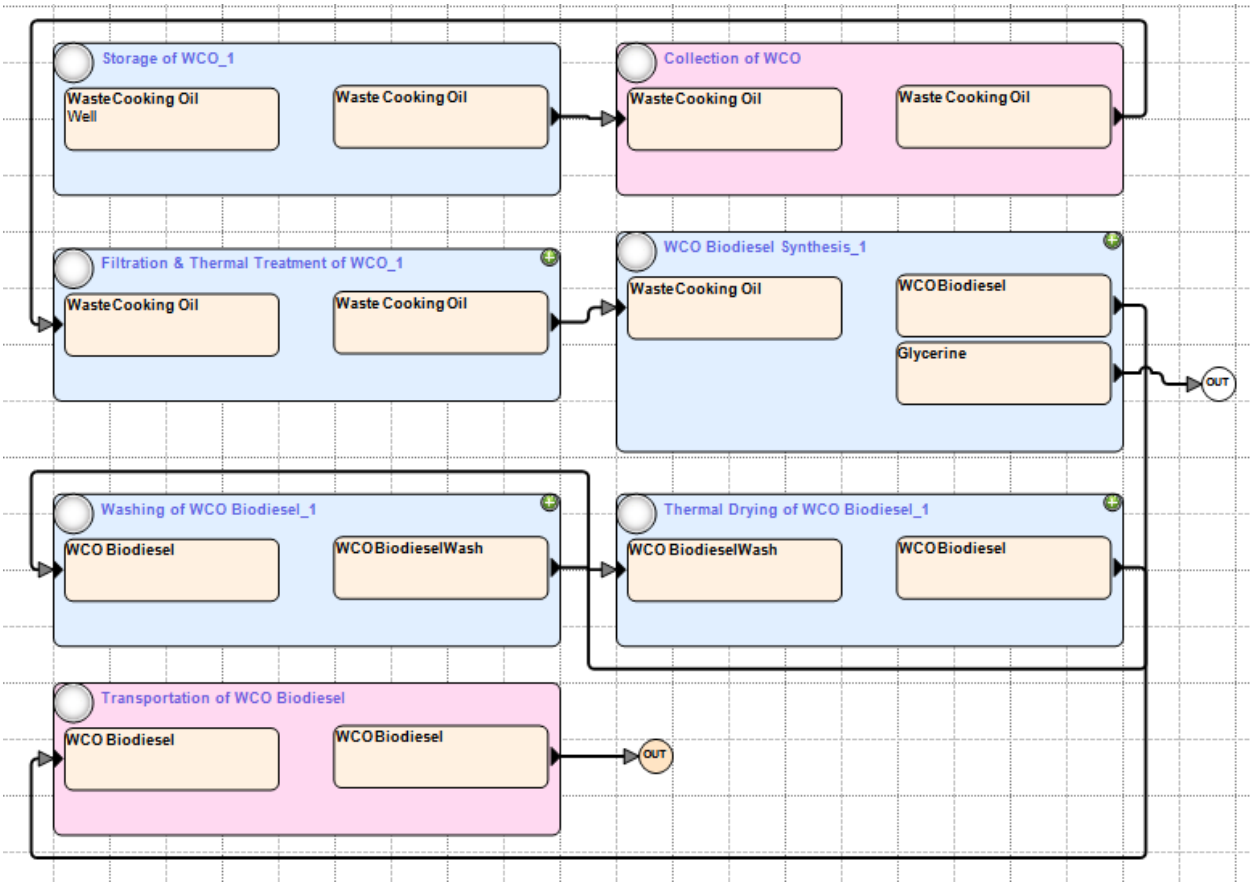

Figure 9. The pathway of production of WCO biodiesel from WCO using GREET model

The functional unit (FU) considered for this analysis is production of 36 gallons of WCO biodiesel for its usage in KU on Wheels buses for on-campus public transportation. The raw material is the used cooking oil that is considered waste from KU dining centers across the campus with its properties given in Figure 2. This WCO is used for the synthesis of biodiesel in a pilot plant on-campus run by the KU Biodiesel Initiative (KUBI).

Table 2. Tabulation of properties used to define new resources in GREET model [6, 54, 55]

Property	WCO	WCO Biodiesel	WCO Biodiesel Wash
Density (kg/m^3)	921.600	878.000	939.000
LHV (MJ/m^3)	33371.136	35018.247	35018.247
HHV (MJ/m^3)	35451.187	36121.893	36121.893
Sulfur Ratio (%)	24.100	7.100	7.100
Carbon Ratio (%)	0.030	0.010	0.010
Market Value ($/gal)	0.000	1.295	1.295

The used cooking oil is considered waste and is collected at all the dining centers for its transportation to the processing unit (KUBI). The storage process is considered stationary according to GREET terminology. Moreover, since WCO is considered as waste, processes upstream are not considered in this analysis and, thus, there is no additional energy consumed and no emissions generated in the storage of WCO [30, 36, 37].

WCO is added to the GREET database as a new resource to enable the model to perform the necessary calculations. A light duty diesel vehicle (LDDV) running on ULSD is used to transport stored WCO from dining centers across the campus to the KUBI pilot plant. Thus, an approximate transportation distance of 6 miles is used since WCO must be gathered at multiple locations. The payload of the mode of transport is defined in GREET to enable the model to calculate emissions for the distance commuted. Of note, the capacity of the pilot plant to process WCO per batch is 41 gallons and this information is included in the transportation analysis.

Table 3. Emissions produced and energy consumed per kg of WCO for each process shown in Figure 9

Species	Storage of WCO	Trans.	Filt/Thrml	Prod.	Wsh/Dry	Filling	Total	Units
VOC	0	43.139	2.928	135.212	104.776	50.329	336.384	mg
CO	0	171.909	2.005	201.021	210.734	200.560	786.229	mg
NO_x	0	361.511	9.628	375.623	428.028	421.762	1596.552	mg
PM_{10}	0	26.319	97.767	119.836	279.271	30.705	553.898	mg
$PM_{2.5}$	0	19.928	28.121	86.976	116.273	23.249	274.547	mg
SO_x	0	34.965	4.234	157.255	115.110	40.792	352.356	mg
CH_4	0	153.826	56.013	924.377	711.112	179.463	2024.791	mg
N_2O	0	425.406	605.331	1337.616	2204.663	496.307	5069.323	ug
CO_2	0	96.731	38.161	172.526	226.609	112.853	646.880	g
Resources	36.21	38.039	0.527	16.673	30.451	2.134	87.824	MJ
Waste Cooking Oil	36.21	0	0	6.021	23.403	0	65.634	MJ
Crude Oil	0	1.058	0.006	0.941	0.760	1.235	4.000	MJ
Water	0	0.475	0.122	1.791	0.566	0.554	3.508	MJ
Natural Gas	0	0.163	0.060	8.129	4.598	0.190	13.140	MJ
Bitumen	0	0.105	0.084	0.029	0.075	0.122	0.415	MJ
Coal Average	0	0.021	0.255	0.608	1.012	0.025	1.921	MJ
Nuclear Energy	0	0.003	0	0.032	0.019	0.004	0.058	MJ
Pet Coke	0	0.002	0	0.002	0.001	0.002	0.007	MJ
Hydroelectric Power	0	0.001	0	0.013	0.008	0.002	0.024	MJ
Wind Power	0	0.001	0	0.004	0.003	0.001	0.009	MJ
Forest Residue	0	0	0	0.002	0.001	0	0.003	MJ

In Table 3, the emissions produced in grams and energy consumed in MJ per kg of WCO output are provided for the transportation pathway. After the stored WCO is transported to KUBI, it is subjected to filtration followed by thermal treatment. In this process, the raw WCO is filtered for particulates with a strainer between a collection tank and a thermal heating tank. After filtration is complete, the output of 40.5 gallons of

WCO is heated to the catalytic reaction temperature of 60°C. Of note, the thermal heating tank is insulated to avoid any heat loss. The energy source used to pump WCO for filtration and thermal heating is electricity produced from coal for local distribution.

Table 4. Emissions produced (g/kg$_{fuel}$) in WtE analysis of WCO biodiesel

Well to Pump (WtP)		Pump to Exhaust (PtE)					WtE
		0.5 N·m	4.5 N·m	9.0 N·m	13.5 N·m	18.0 N·m	18.0 N·m
VOC	0.336	2.461	0.926	0.445	0.292	0.190	0.526
CO	0.786	29.201	12.676	5.510	3.789	3.575	4.361
NO_x	1.597	14.284	14.639	13.132	11.780	12.023	13.62
PM	0.829	0.008	0.032	0.119	0.279	0.933	1.762
SO_x	0.352	0.094	0.031	0	0	0.030	0.382
CH_4	2.025	0.149	0.072	0.046	0.035	0.022	2.047
N_2O	0.005	0.089	0.064	0.043	0.030	0.024	0.029
CO_2	646.88	1408.792	1424.734	1400.816	1395.41	1392.985	2039.865

A schematic representation of details of the entire production pathway with all the inputs, outputs, and energy supplied are used in GREET to model all the stationary processes as shown in Figure 10. This allows the model to estimate the overall energy used and emissions produced during filtration and thermal treatment provided in Table 3.

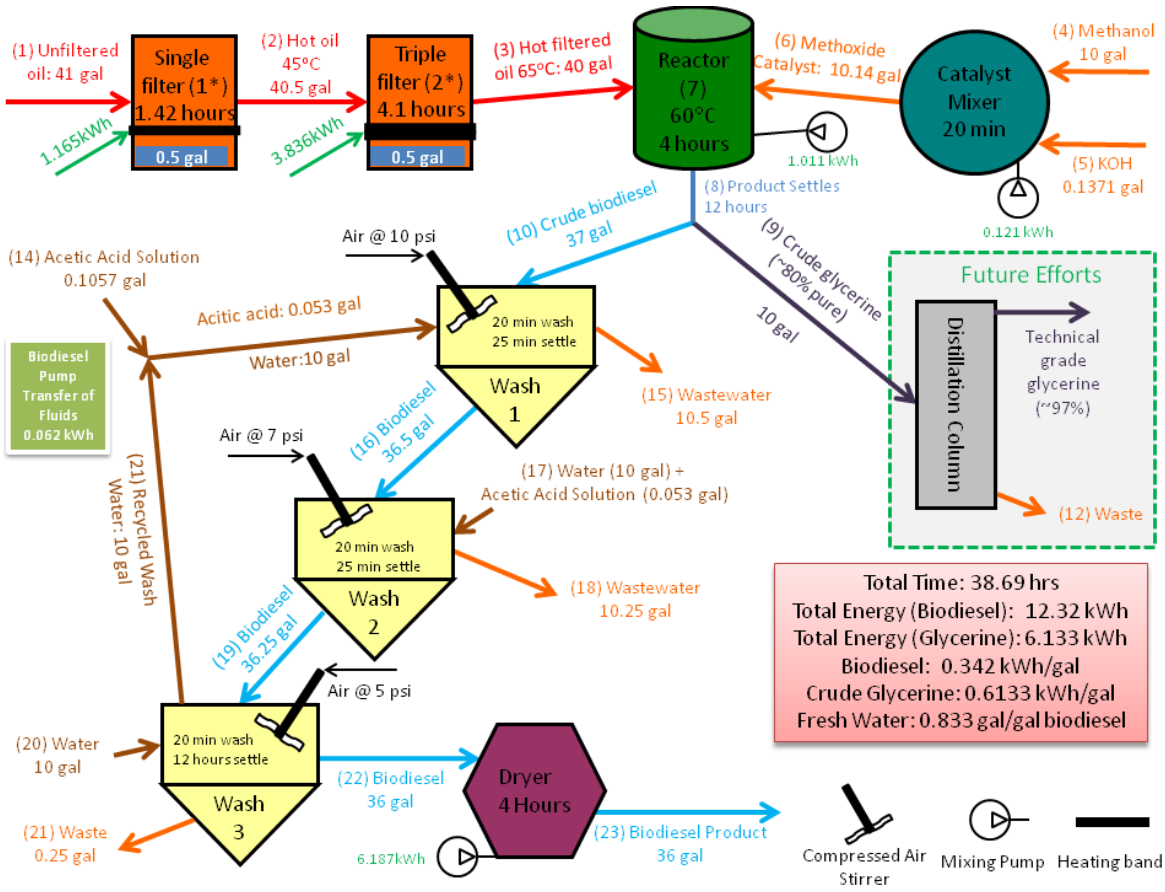

Figure 10. Schematic diagram describing the production of WCO biodiesel [46]

After thermal treatment, 36 gallons of WCO biodiesel is synthesized by alkali-catalyzed transesterification of 40 gallons of WCO with methanol and potassium hydroxide as the catalyst materials. The molar ratio used for the synthesis reaction is 4:1 between WCO and methanol, respectively. For 40 gallons of WCO, 10 gallons of methanol is utilized along with 1100 gm of potassium hydroxide. The potassium hydroxide is mixed with methanol prior to its addition to the reactor unit with 40 gallons of WCO. The entire mixture is stirred continuously at the reaction temperature for 4 hrs. The resulting products of this catalytic reaction are WCO biodiesel and glycerin. The quantity of the WCO biodiesel is 36 gallons as final output per batch.

To outline this process in Figure 10, WCO biodiesel has to be defined as a resource in GREET employing its properties in Figure 2. The default GREET properties for methanol (generated from US produced natural gas) and potassium hydroxide resources are used in the analysis. In addition, the energy input needed to maintain the reactor temperature at 60°C and to stir the mixture inside the reactor for 4 hrs are defined including their corresponding shares of energy source (i.e., coal power plant). This helps the model estimate the energy consumed and emissions involved up until this process as shown in Table 3.

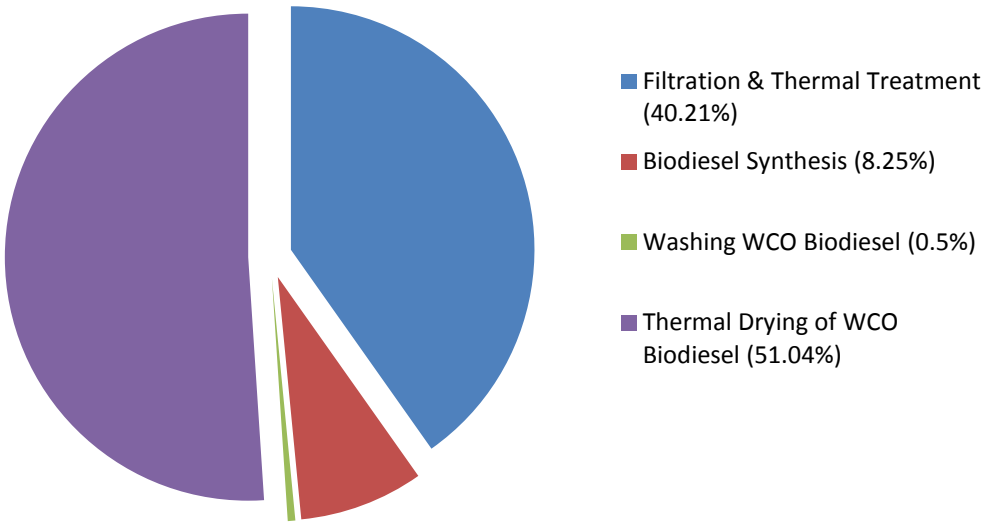

Figure 11. The usage of energy during all the stationary processes of production pathway

Subsequently, WCO biodiesel is washed with 10 gallons of water and 200 ml of acetic acid in two successive cycles in order to separate the biodiesel product from unreacted methanol. The resulting mixture is then washed again using only 10 gallons of water. The wastewater from biodiesel washing process is recycled for its use in next

cycle as shown in Figure 10. The output of this final wash is subjected to thermal drying in order to obtain the required product. In specific, the difference in heats of vaporization of water, acetic acid, and WCO biodiesel leads to the collection of a relatively pure WCO biodiesel product. The percentages of energy consumed for each process in production pathway are shown in Figure 11. This product, known in GREET as WCO biodiesel wash, is defined as a new resource (see Figure 2) to account for any potential changes in the properties of the mixture. In addition, the energy input for thermal drying is defined alongside the definition of this new energy source. Figure 9 provides the GREET model for this washing and drying process with the subsequent emissions shown in Table 3.

Finally, the obtained product of 36 gallons of WCO biodiesel is transported to the filling station of KU on Wheels by a LDDV (using ULSD) as illustrated in the GREET model via Figure 9. The approximate distance considered for the transportation is 6 miles. This transportation process contributes to the overall emissions produced. The payload of this transportation process is defined in order to enable the model to approximate emissions for changes in payload as shown in Table 5.

Pump to Exhaust (PtE) analysis on a $g_{emissions}/kg_{fuel}$ basis is performed using single cylinder compression ignition engine test data of WCO biodiesel over the entire engine load range as shown in Table 4. Combining this information with the WtP data into a WtE analysis suggests that the PtE emissions of CO, CO_2, and NO_x contribute significantly to overall emissions of the fuel. A more thorough discussion of these results will follow the WPF LCA in order to compare and contrast the different fuels. Of note, PM emissions data from the engine test cell cannot be discerned in regards to the 2.5 μm and 10 μm level. Hence, a single value in the 10 μm row is presented for PM in Table 4

for PtE emissions while both PM values are summed to represent PM emissions for WtP emissions.

Table 5. Shows changes in payload during both the transportation process

Transportation Process	Payload
Collection of WCO (40 gal)	140.0 kg
Transportation of WCO biodiesel (36 gal)	120.0 kg

3.6 WtE Analysis of Waste Plastic Fuel (WPF)

The WtE analysis for WPF is performed similar to that of WCO biodiesel. However, the well to pump analysis is now accomplished by approximating a model based on the literature review while the pump to exhaust analysis is derived from the efforts of Chapter 2. The well to pump analysis of WPF consists of following processes:

- Storage of PSW
- Transportation of PSW
- Cleaning and Drying of PSW
- Shredding of PSW
- Thermal Pyrolysis of PSW
- Cooling and Distillation of Pyrolysis Gas
- Transportation of WPF

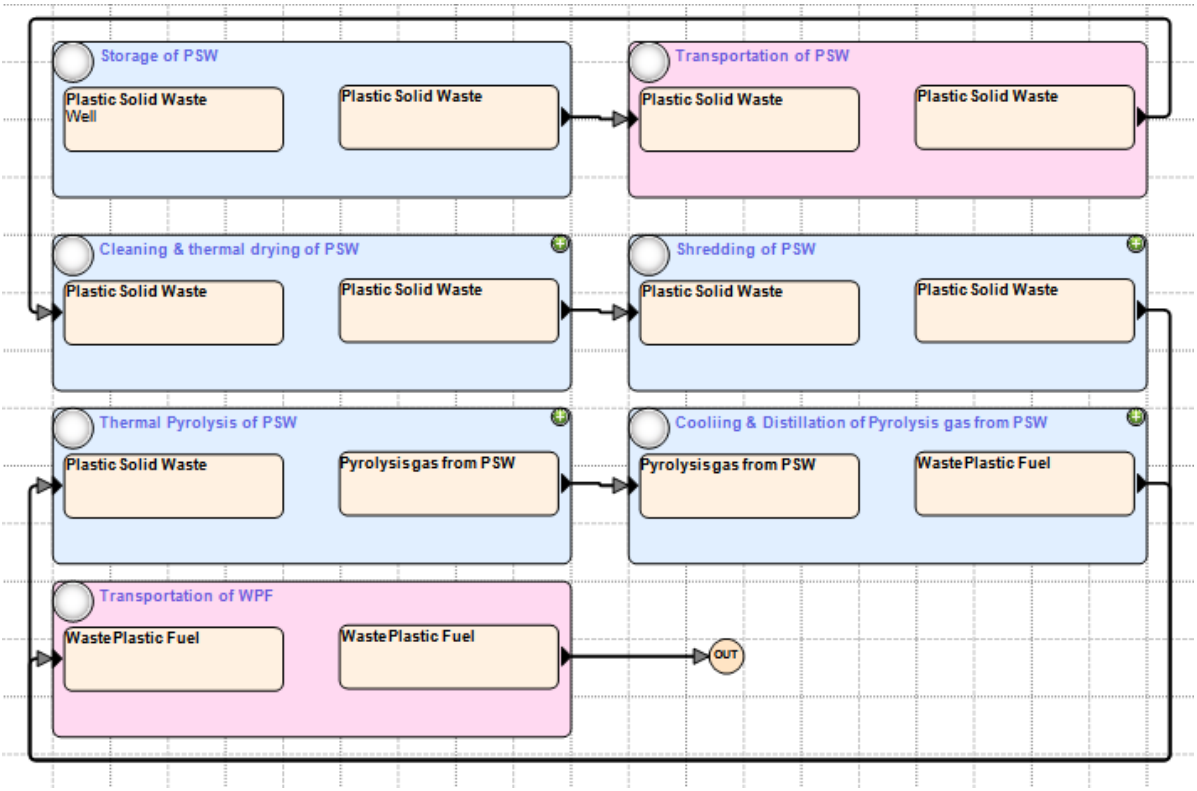

Figure 12. Pathway of synthesis of waste plastic fuel (WPF) from plastic solid waste (PSW)

The FU considered for this analysis is 36 gallons of output fuel in order to compare emissions and energy consumed during the LCAs of WPF and WCO biodiesel similarly. Analogous to WCO biodiesel, WPF is produced for utility in on-campus public transportation. The raw material used is PSW that is collected periodically by KU Recycling from numerous locations on campus with its properties given in Table 6. Estimates from KU Recycling state that about 3.15 tons of PSW is collected on average every month. This collected PSW is subjected to thermal pyrolysis using approximate process conditions found in the literature while employing a hypothetical laboratory on campus. The energy supply to run the production pathway is considered to be electricity produced from a coal thermal plant for domestic use in Lawrence, KS.

The majority of the PSW is segregated from MSW at the trashcan since each recycling container is clearly labeled for particular types of waste across the campus. The collected trash is transported to the KU Recycling unit from all buildings across campus. At the recycling unit, the PSW is further segregated from MSW and accumulated to feed into the WPF production pathway. The transportation distance to move waste from all across the campus to the recycling unit is normalized to 16 miles as that of collection of WCO for proper LCA comparison of both fuels. In other words, the transportation distance between WCO and WPF feedstock has been equated in order to provide the same amount (36 gallons) of resultant fuel.

Table 6. Tabulation of properties used to define new resources in GREET model [54, 55]

Property	PSW	WPF
Density (kg/m^3)	1096.30	800.70
LHV (MJ/m^3)	32179.91	37066.00
HHV (MJ/m^3)	34395.71	39281.80
Sulfur Ratio (%)	0.00	0.00
Carbon Ratio (%)	0.10	0.00

The PSW and WPF are defined as new resources in GREET model using the properties shown in Table 6. Since PSW is considered as waste with no value, processes upstream of the storage of PSW are not included in this analysis as shown in Figure 12. Similar to the collection of WCO, a LDDV running on ULSD is used in the collection of PSW. Because the FU is fixed to 36 gallons of output fuel to compare both fuel pathways directly, the quantity of feedstock is reverse engineered to be 133.0673 kg of PSW based on the approximate yield percentage of required liquid fuel (82%) while the rest of the

yield (18%) is gaseous fuel on mass basis. The calculated liquid and gas yields are shown in Table 7 based on fixed FU.

Table 7. Calculation of respective liquid and gas yields from fixed FU

Mass basis FU (WPF)	109.1152 kg
Liquid Yield (WPF)	82 %
Req. feedstock (PSW)	133.0673 kg
Gas yield (syngas/producer gas)	18 %
Syngas/producer gas	23.952 kg

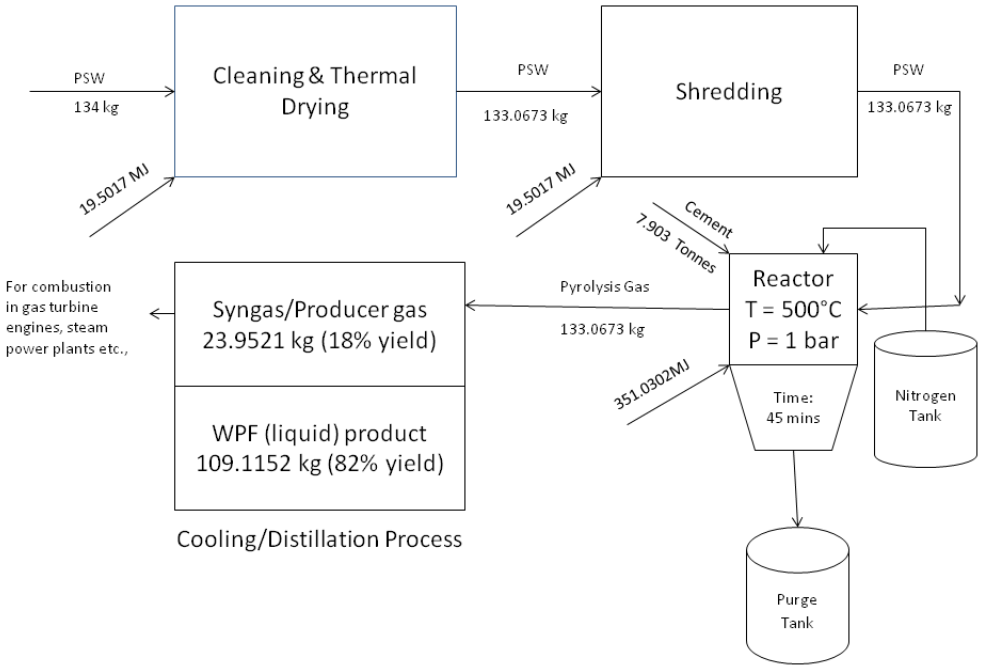

Figure 13. Schematic representation of approximate synthesis technique of WPF by not using co-produced syngas as a supplemental energy source

The approximate synthesis technique used to model the well to pump LCA analysis of waste plastic fuel is thermal pyrolysis for its simplicity and from available information [50, 51, 53, 54]. Here, this synthesis technique is scaled up from a pilot plant running on 10 gm of PSW feedstock to yield a normalized 36 gallons of fuel for proper comparison to WCO biodiesel. This process is carried out in a cement bed reactor to

maximize liquid yield (WPF). This cement is assumed to not be consumed over the reaction process and it helps to maintain the reaction temperature by dissipating heat to the feedstock uniformly from the heat source. Two different setups are simulated for this process where syngas/producer gas is not used or used as a supplemental energy source for heating requirements of the reactor, respectively. A schematic representation of synthesis technique where syngas is not used as supplemental energy source in production pathway is shown in Figure 13. In this production pathway, the feedstock (PSW) is subjected to flush water cleaning followed by drying to get rid of the dust and particulates. The output of this process is considered the calculated PSW of 133.0673 kg that is further subjected to shredding to sizes 4-5 mm in diameter. The shredded feedstock material is now conveyed to the reactor followed by the addition of reactor bed material and is stirred to achieve uniform mixture. The shredding of the feedstock material improves the surface area of the feedstock material and allows the reactor bed material (cement) to aid in uniform heat distribution. Nitrogen is used to purge the reactor from any available air to purge tank for 10 min at the rate of 0.2 L/min as shown in Figure 13. The reactor is now heated to a reaction temperature of 500°C and this temperature is maintained for 45 minutes using only electric heaters.

Table 8. Emission produced and energy consumed during WtP analysis of WPF via synthesis technique shown in Figure 13

Species	Storage of PSW	Trans.	Cleaning, Drying, & Shredding	Thermal Pyrolysis	Cooling & Distillation	Filling	Total	Units
VOC	0	120.189	7.511	60.017	41.21	54.904	283.831	mg
CO	0	478.95	7.923	41.096	115.908	218.793	862.67	mg
NO_x	0	1007.194	28.99	197.378	270.81	460.104	1964.476	mg
PM_{10}	0	73.326	223.208	2004.242	505.1	33.497	2839.373	mg
$PM_{2.5}$	0	55.52	64.443	576.484	152.894	25.362	874.703	mg
SO_x	0	97.415	10.327	86.793	42.707	44.501	281.743	mg
CH_4	0	428.569	130.592	1148.291	374.845	195.778	2278.075	mg
N_2O	0	1185.211	1387.138	12409.46	3289.023	541.426	18812.26	ug
CO_2	0	269.5	88.813	782.318	250.408	123.113	1514.152	g
Resources	29.311	3.774	1.154	8.291	9.337	1.724	53.591	MJ
Plastic Solid Waste	29.311	0	0.205	0	6.48	0	35.996	MJ
Crude Oil	0	2.949	0.033	0.115	0.68	1.347	5.124	MJ
Natural Gas	0	0.454	0.007	0.027	0.107	0.207	0.802	MJ
Bitumen	0	0.291	0.004	0.011	0.067	0.133	0.506	MJ
Coal Average	0	0.059	0.904	8.133	1.997	0.027	11.12	MJ
Nuclear Energy	0	0.01	0	0.003	0.003	0.004	0.02	MJ
Pet Coke	0	0.005	0	0	0.001	0.002	0.008	MJ
Hydroelectric Power	0	0.004	0	0.001	0.001	0.002	0.008	MJ
Wind Power	0	0.001	0	0	0	0.001	0.002	MJ
Forest Residue	0	0.001	0	0	0	0	0.001	MJ

The output of this process is called a pyrolysis gas with a mixture of lighter and heavier hydrocarbons subsequently subjected to distillation in order to collect WPF as main liquid product and syngas/producer gas co-product. The co-produced syngas/producer gas is used for combustion in gas turbine engines and steam power plants. Unfortunately, not enough information exists as to the standardized species profile of this syngas to add it to the LCA. Therefore, similar to the glycerin derived from the WCO biodiesel, it is not included in the first WPF production analysis. Hence, the LCA

described for both fuels (WPF and WCO biodiesel) concentrates on the main products of interest (and main outcome of combustion in a CI engine) while leaving the co-product LCAs for a future effort once more information can be gathered.

The input and output mass is assumed to be equivalent between shredding, thermal pyrolysis, and distillation processes. The energy input for the entire production pathway is assumed to be 10% of the total energy content of the feedstock based on the literature [13, 15, 16]. The usage of energy during all the stationary processes are shown in Figure 14 as a function of total energy consumed for the production pathway. The energy consumed, inputs, and output masses during all the stationary processes are shown in Figure 13 that are fed into GREET model to evaluate emissions produced and energy consumed for WtP analysis for this setup as shown in Table 8.

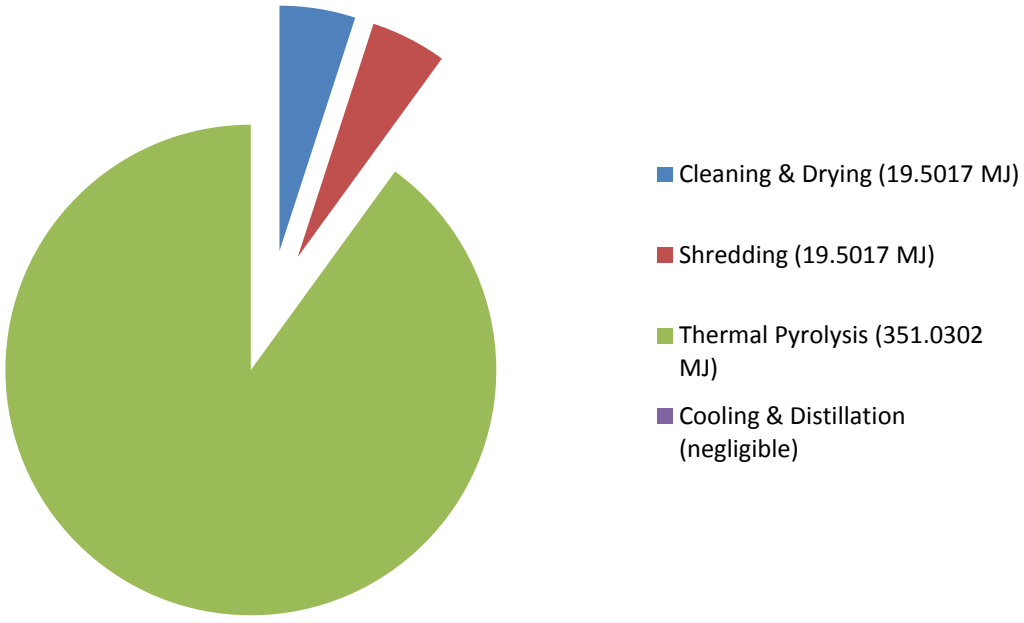

Figure 14. The usage of energy during all the stationary processes of production pathway for WPF

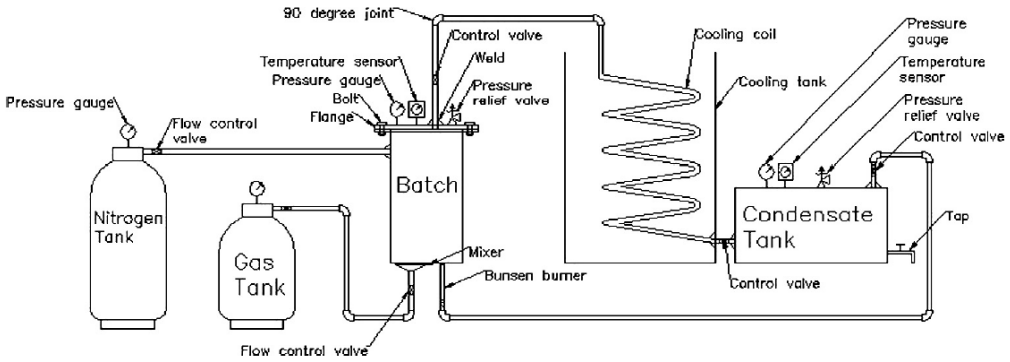

Figure 15. Experimental setup of a model thermal pyrolysis process for WPF [52]

Now, the thermal pyrolysis technique is discussed with a slight change in setup where the co-produced syngas/producer gas is used as a supplemental source of energy to provide for heating requirements of the reactor as shown in Figure 15. The only difference in this experimental setup includes changes in energy inputs. This co-product saves about 78.28% of the total energy consumed for production pathway. The usages of energy by all the processes involved in the production pathway are updated in Figure 17 for this new configuration. The purpose and methodology involved in all the stationary processes are same as the previous setup discussed earlier.

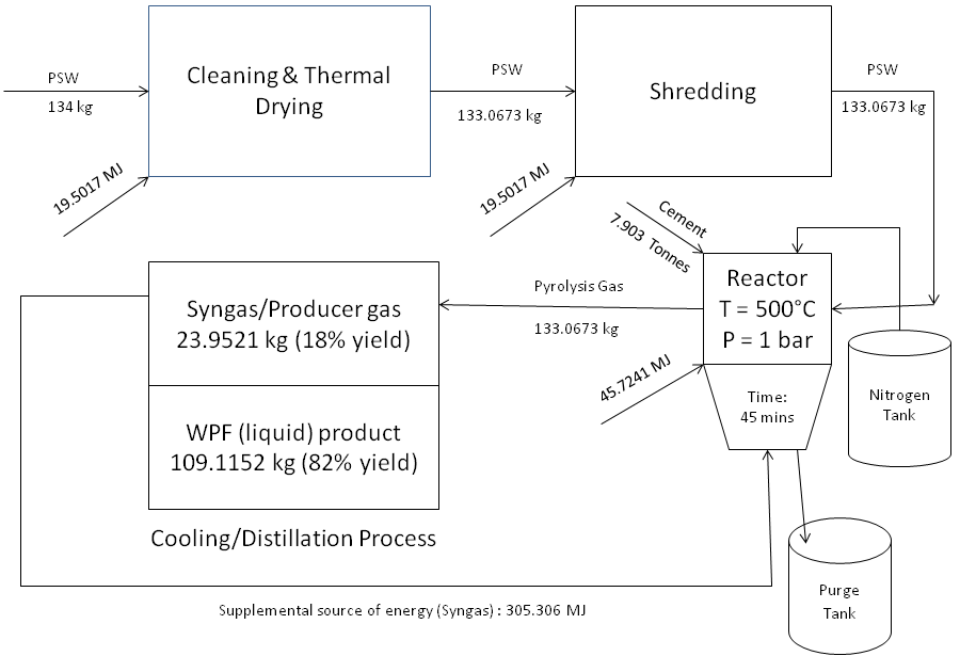

Figure 16. Schematic representation of production of WPF with syngas/producer gas as supplemental energy resource

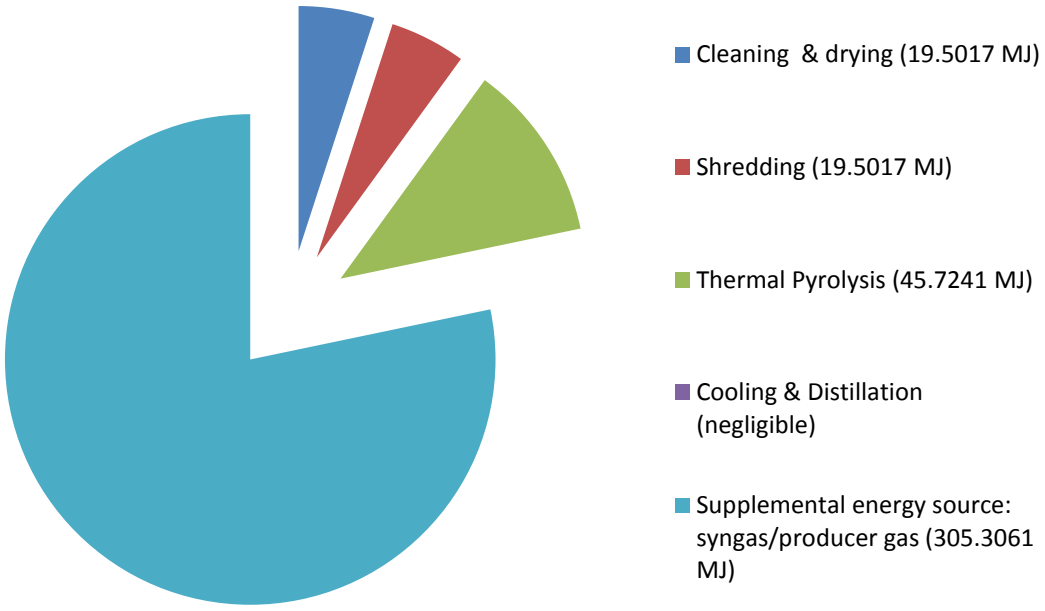

Figure 17. The usage of energy during all the stationary processes of production pathway of WPF

The energy consumed, input, and output masses in each process are shown in a schematic representation of production pathway in Figure 16. These values are fed into the GREET model to evaluate for emissions produced and energy consumed during WtP analysis as shown in Table 9.

Table 9. Emissions produced and energy consumed per kg of WPF for each process shown in Figure 16

Species	Storage of PSW	Trans.	Cleaning, Drying, & Shredding	Thermal Pyrolysis	Cooling & Distillation	Filling	Total	Units
VOC	0	120.189	7.511	7.818	29.751	54.904	220.173	mg
CO	0	478.95	7.923	5.353	108.061	218.793	819.08	mg
NO_x	0	1007.194	28.99	25.71	233.122	460.104	1755.12	mg
PM_{10}	0	73.326	223.208	261.066	122.413	33.497	713.51	mg
$PM_{2.5}$	0	55.52	64.443	75.091	42.821	25.362	263.237	mg
SO_x	0	97.415	10.327	11.305	26.135	44.501	189.683	mg
CH_4	0	428.569	130.592	149.573	155.591	195.778	1060.103	mg
N_2O	0	1185.211	1387.138	1616.417	919.579	541.426	5649.771	ug
CO_2	0	269.5	88.813	101.902	101.033	123.113	684.361	g
Resources	29.311	3.774	1.154	1.08	7.753	1.724	44.796	MJ
Plastic Solid Waste	29.311	0	0.205	0	6.48	0	35.996	MJ
Crude Oil	0	2.949	0.033	0.015	0.658	1.347	5.002	MJ
Natural Gas	0	0.454	0.007	0.004	0.102	0.207	0.774	MJ
Bitumen	0	0.291	0.004	0.001	0.065	0.133	0.494	MJ
Coal Average	0	0.059	0.904	1.059	0.444	0.027	2.493	MJ
Nuclear Energy	0	0.01	0	0	0.002	0.004	0.016	MJ
Pet Coke	0	0.005	0	0	0.001	0.002	0.008	MJ
Hydroelectric Power	0	0.004	0	0	0.001	0.002	0.007	MJ
Wind Power	0	0.001	0	0	0	0.001	0.002	MJ
Forest Residue	0	0.001	0	0	0	0	0.001	MJ

As mentioned prior, it is assumed that the solid residue formed during both the setups of synthesis techniques is negligible in mass with respect to the resulting products. The main output from both the setups is further transported to filling stations using a

LDDV for on-campus public transportation. The transportation distance from KU recycling unit to fuel filling stations is approximated to be 6 miles using Google maps. The payload of both the transportation processes in the production pathway is defined to enable the model to approximate emissions for changes in payloads as shown in Table 7. The production pathways are created with above mentioned processes with all the input parameters defined in Figure 13 and Figure 16 to enable the GREET model to estimate energy consumed and emissions produced during entire production pathways and individual processes with different setups as discussed earlier are shown in Table 8 and Table 9, respectively.

Table 10. Shows changes in payload during both the transportation process

Transportation Process	Payload
Collection of PSW	134 kg
Transportation of WPF (36 gallons)	110 kg

On comparing the LCA of WtP analysis results between both the experimental setups suggest that the setup with the use of co-produced syngas/producer gas as supplemental energy resource is proven to be a relatively more sustainable approach with respect to emissions produced and energy consumed during the entire production pathway as shown in Figure 16. Thus, results from WtP analysis of this particular setup as shown in Table 9 are chosen over the former to perform WtE analysis of WPF in Table 11 for comparison to WCO biodiesel and ULSD.

Table 11. WtE emissions produced (g/kg_{fuel}) for production and use of WPF

Wheel to Pump (WtP)			Pump to Exhaust (PtE)					WtE
	Table 5	Table 6	0.5 N·m	4.5 N·m	9.0 N·m	13.5 N·m	18.0 N·m	18.0 N·m
VOC	0.284	0.220	3.162	1.117	0.603	0.417	0.302	0.522
CO	0.863	0.819	32.984	14.616	7.299	5.003	4.969	5.788
NO_x	1.964	1.755	18.413	18.149	16.946	15.803	17.492	19.247
PM	3.714	0.977	0.033	0.165	0.487	0.734	1.728	2.705
SO_x	0.282	0.19	0.165	0.000	0.000	0.007	0.029	0.219
CH_4	2.278	1.06	0.171	0.087	0.057	0.033	0.02	1.08
N_2O	0.019	0.006	0.109	0.082	0.056	0.042	0.032	0.038
CO_2	1514.152	684.361	2149.93	2187.859	2177.217	2097.146	2111.048	2795.409

3.7 WtE Comparison Between WCO Biodiesel, WPF, and ULSD

The LCA for the WtP analysis of ULSD is performed using a predefined pathway for production of low sulfur diesel from crude oil [56, 57] by normalizing the input parameters to generate a FU of 36 gallons of output fuel. The emissions produced and energy consumed during this WtP analysis is shown in Table 12. Of note, the ULSD PtE information comes from the same experiments as the previous chapter (i.e., baseline tests prior to running WPF).

Table 12. WtE emissions produced (g/kg_{fuel}) for production and use of ULSD

Wheel to Pump (WtP)		Pump to Exhaust (PtE)					WtE
		0.5 N·m	4.5 N·m	9.0 N·m	13.5 N·m	18.0 N·m	18.0 N·m
VOC	0.295	8.044	1.872	0.743	0.416	0.283	0.578
CO	0.539	80.09	30.407	12.815	6.824	5.575	6.114
NO_x	1.461	18.047	22.853	21.338	19.094	18.442	19.903
PM	0.403	0.010	0.022	0.149	0.440	1.945	2.348
SO_x	0.840	0.536	0.085	0.041	0.040	0.057	0.897
CH_4	5.684	0.385	0.124	0.059	0.035	0.022	5.706
N_2O	0.004	0.096	0.083	0.056	0.043	0.035	0.039
CO_2	546.238	2074.954	2151.923	2178.474	2184.086	2200.066	2746.304

Table 13. Comparison of WtP emissions produced for WCO biodiesel, WPF, and ULSD on a g/kg$_{fuel}$ basis with highest value for each row in bold

WtP	ULSD	WPF	WCO Biodiesel
VOC	0.295	0.220	**0.336**
CO	0.539	**0.819**	0.786
NO_x	1.461	**1.755**	1.597
PM	0.403	**0.977**	0.829
SO_x	**0.840**	0.190	0.352
CH_4	**5.684**	1.060	2.025
N_2O	0.004	**0.006**	0.005
CO_2	546.238	**684.361**	646.880

The WtP emissions produced for WCO biodiesel, WPF, and ULSD are presented in Table 13 to illustrate the difference in emissions across the production pathways of these three fuels at the highest engine load setting. The VOC emissions are observed to be relatively lower for the WtP analysis of WPF in comparison to WCO biodiesel and ULSD. This is believed to be because WPF is a solid feedstock in comparison to liquids for the other sources. Hence, there is less likelihood of VOC emissions during its transport and conversion. WCO biodiesel has the highest VOC production because methanol used in the production pathway is relatively more volatile than ULSD.

In addition, the CO, NO_x, and PM emissions produced during the WtP analysis are observed to be relatively higher for WPF as compared to WCO biodiesel and ULSD. This could be attributed to the relative amounts of electrical energy consumed to fuel the respective production pathways. In this effort, the geographic location (Lawrence, KS) requires the use of a coal thermal power plant. This is defined in GREET as a pathway mix to account for emissions produced during electrical energy production. The WPF production pathway is observed to consume the highest amount of electrical energy at 40.673% and 80.836% more energy than the WCO biodiesel and normalized ULSD production pathways, respectively.

Furthermore, the SO_x emissions from WtP analysis are observed to be relatively higher for ULSD followed by WCO biodiesel and WPF due primarily to the sulfur content of the feedstock material. In specific, ULSD is observed to have relatively higher sulfur content from its petroleum source followed by that of WCO biodiesel and WPF, respectively. Of note, SO_x emissions from thermal power plants do play into WPF potentially having a higher level of SO_x emissions than WCO biodiesel; however, it appears that the sulfur content of the WCO pathway has a dominating influence leading to relatively higher SO_x emissions for WCO biodiesel than WPF.

The CH_4 emissions are observed to be the highest for ULSD followed by WCO biodiesel and WPF, respectively. This is due to the corresponding amounts of natural gas consumed directly or indirectly. The normalized ULSD production pathway consumes significant amounts of natural gas directly while the WCO biodiesel production pathway consumes natural gas in an indirect manner from its methanol usage (25% of the feedstock material by volume). The amount of CH_4 emissions during the WtP analysis of WPF are due to the consumed electrical energy produced from coal thermal plants. Moreover, the primary contributor of CO_2 and N_2O emissions is the respective transportation process followed by use of electrical energy for feedstock conversion purposes. The WtP analysis suggests the WPF production pathway sees the highest CO_2 and N_2O emissions followed by WCO biodiesel and ULSD, respectively, because the normalized transportation distance and electrical energy consumed are in the following order WPF > WCO biodiesel > ULSD. ULSD is lowest here because of the scale of its production. The transportation of ULSD from Well to Pump involves massive amounts of feedstock and fuel being moved by ocean-going barges, rail car, etc. In comparison, the

transportation of WCO biodiesel and WPF is a localized and relatively inefficient process (i.e., moving small batches). Hence, growing these fuels on a massive scale would see their CO_2 and N_2O emissions drop from a WtP perspective.

Based on the WtP analysis, WCO biodiesel is observed to have a relatively better LCA as compared to ULSD and WPF (thermal) production pathways. However, because the WPF tested in the previous chapter did employ a catalytic conversion process, the results presented here are (most likely) the worst-case scenario for WPF conversion. Hence, it is expected that its WtP LCA is the respective best as employing a catalytic process will reduce conversion time while also employing lower temperatures resulting in reduced electrical energy consumption and the lowest emissions. Of note, employing residual methanol recycling in the current production pathway of WCO biodiesel may lower CH_4 emissions.

Of note, since WPF and biodiesel fuels have been compared to ULSD via prior PtE efforts (previous chapter and [58], respectively), ULSD will not be discussed in the PtE analysis presented here. Investigating the emissions produced during combustion of WPF in comparison to WCO biodiesel in Table 4 and Table 11, one sees relatively higher emissions for WPF across all engine loads. In order to discuss the PtE analysis further, their respective fuel properties are compared as shown in Table 14.

Table 14. Comparison of fuel properties of WCO biodiesel and WPF [6]

Property	WCO Biodiesel	WPF	ULSD
Density (kg/m^3)	878	800	841
Kinematic Viscosity (cSt)	4.85	2.97	2.74
Dynamic Viscosity (cP)	4.25	2.33	2.31
Cetane Number (CN)	52.80	71.88	48.61
Energy Content (kJ/kg)	36210	46292	45670
Energy Content (MJ/m^3)	31792	37066	38423

The relatively higher viscosity of WCO biodiesel suggests that it is more difficult to atomize the fuel leading to poorer fuel and air mixture preparation as compared to that of WPF. In addition, its lower cetane number suggests a longer ignition delay. Furthermore, the energy content of WCO biodiesel is lower on volumetric basis despite having a higher density. Since the fuel injection system adds fuel on a volumetric basis, comparing WCO biodiesel to WPF:

- Higher viscosity = less fuel prepared for pre-mixed combustion
- Lower cetane number = more fuel prepared for pre-mixed combustion
- Lower volumetric energy = less fuel energy for pre-mixed combustion

These findings suggest that WCO biodiesel would have a lower pre-mixed combustion phase (i.e., less constant volume combustion leading to lower temperatures and NO_x emissions) and greater diffusion burn phase (i.e., air limited combustion leading to greater CO/HC/PM emissions). However, given the significantly higher cetane number of WPF, it is possible that levels of pre-mixed combustion are nearly equivalent. Overall, based only on fuel properties, for WCO biodiesel one would expect lower NO_x emissions (seen), higher CO/HC/PM emissions (not seen), and worse fuel economy leading to higher CO_2 emissions (not seen) given the reduced fuel energy available and comparatively worse mixing. It is important to mention that if fuel consumption (i.e., brake specific fuel consumption - bsfc) is significantly better for WPF versus WCO biodiesel, because the analysis is presented on a g/kg_{fuel} basis the emissions results may appear worse for WPF. Hence, less WPF is needed to generate the needed power and the overall total mass of emissions is less. At 18.0 N·m, the respective bsfc values for WPF

and WCO biodiesel are 236.029 and 273.793 g_{fuel}/kWh indicating that this is indeed a potential factor.

Further deviations from the expected trends may result from the respective fuel chemistry effects between the two fuels. In specific, the chemical makeup of WCO biodiesel is known [8]; whereas, the relative level of saturation and unsaturation is unknown for WPF. However, it can be assumed that WPF does not contain significant quantities of oxygen unlike WCO biodiesel. Therefore, the lower CO, HC, and PM emissions of WCO biodiesel can be explained because the embedded oxygen promotes complete combustion. Moreover, from the CO_2 results, it appears that the chain length of WPF is significantly longer and more carbon bonds exist in the fuel. However, further fuel chemistry analysis is needed to completely understand the results.

Table 15. Comparison of WtE emissions produced for WCO biodiesel, WPF, and ULSD

WtE	ULSD	WPF	WCO Biodiesel
VOC	**0.578**	0.522	0.526
CO	**6.114**	5.788	4.361
NO_x	**19.903**	19.247	13.620
PM	2.348	**2.705**	1.762
SO_x	**0.897**	0.219	0.382
CH_4	**5.706**	1.080	2.047
N_2O	**0.042**	0.038	0.029
CO_2	2746.304	**2795.409**	2039.865

Similar to the WtE analysis performed for WCO biodiesel, a WtE analysis for WPF in Table 11 is performed by retrieving the test data from the efforts of Chapter 2 and using it in conjunction with WtP analysis performed using the GREET model results of Table 9. The emissions produced during WtE analysis of test fuels shown in Table 15 are a direct summation of corresponding results of WtP analysis and PtE analysis at full

load. On comparing the results of WTE analysis, the LCA of WCO biodiesel is observed to be relatively lower as compared to WPF and ULSD for the majority of the categories. The LCA of WtP analysis and PtE analysis of this fuel could further be improved by employing the modification to production pathway mentioned prior and by employing higher injection pressures to match the peak in-cylinder pressures of corresponding ULSD baseline test at normalized injection timing. This is the subject of the next chapter.

3.8 Conclusion

In this work, the well-to-exhaust analysis of test fuels is performed under similar conditions. All the production pathways are modeled and normalized to a functional unit of 36 gallons of output fuel for ideal comparison between test fuels. Life Cycle Analysis of fuels from well to exhaust is performed to compare test fuels (WCO biodiesel and WPF) against commercial diesel fuel (ULSD) on the basis of overall emissions produced during creation and combustion. The WtE analysis is performed for WCO biodiesel and WPF by summation of results from WtP using the ANL GREET tool and PtE results from Chapter 2 and concurrent efforts. On comparing the results of WtE analysis, the LCA of WCO biodiesel is observed to be relatively lower as compared to WPF and ULSD. The emissions produced in the WtE analysis of WPF illustrate that the emissions produced during the production pathway (i.e., WtP) are typically higher than that of WCO biodiesel. The emissions produced in the WtP analysis of production pathway of WPF where co-produced syngas is used as supplemental energy source saw significant drop in emissions compared to the pathway otherwise. In addition, the majority of the emissions from WtP analysis of test fuels came from production of electrical energy used in the production pathways. Based on the geographic location, used electrical energy is

defined as produced from coal thermal plant as in Lawrence, Kansas. Furthermore, these emissions could be lowered significantly if electrical energy used to power production pathways comes from clean energy sources like wind, solar etc.

The emissions produced during WtP analysis could further be improved by employing appropriate modifications to production pathways. For example, residual methanol used in the production of WCO biodiesel could be recycled to reduce methane emissions. Furthermore, the emissions produced during PtE analysis could be improved by employing higher injection pressures to attempt to match the peak in-cylinder pressures of corresponding ULSD baseline test at normalized injection timing by negating the influence of relatively high viscosity of WCO biodiesel and WPF.

Chapter IV: Effect of Injection Pressure on the Performance and Emission Characteristics of Waste Cooking Oil Biodiesel

4.1 Introduction

From the efforts of the previous chapter, the emissions produced during the Well to Exhaust (WtE) analysis shows relatively lower emissions for Waste Cooking Oil (WCO) biodiesel as compared to Waste Plastic Fuel (WPF) and Ultra Low Sulfur Diesel (ULSD) for most categories. The goal of the current study is to investigate the Pump to Exhaust (PtE) outcomes of WCO biodiesel fuel by changing injection pressure and potentially further enhance the prior WtE outcomes. This fuel is chosen due to its availability on campus and the inherent advantages of biodiesel with regards to its relatively lower PtE emissions as compared to ULSD [58] at a cost of higher fuel consumption at the same injection pressure. In addition, production of biodiesel from virgin oils has led to significant costs with respect to production of raw materials. Thus, the use of low-cost feedstock, such as WCO, has drawn significant interest to make biodiesel more competitive to diesel fuel. This technique solves the disposal issues of WCO while lowering the cost of biodiesel production significantly [1-3, 9].

4.2 Literature Review

Several prior studies have suggested that atomization, vaporization, mixing, distribution, and combustion of the injected biodiesel fuel could be improved by changing the fuel injection timing [1-3, 59-61], pressure [1, 3, 60-68], profile [68], and duration in a compression ignition (CI) engine. In a previous work by Mattson et al., a

fuel injection timing sweep using ULSD was accomplished using the same engine setup as the author while measuring fuel consumption and emissions. In Mattson et al.'s effort, the fuel injection pressure was held constant and by adjusting injection timing, the authors found an injection crank angle for peak operational efficiency (maximum brake torque, or MBT), wherein Brake Specific Fuel Consumption (BSFC) was minimized in order to meet a given engine load. In addition, it was found that there existed an "envelope" of peak engine performance centered on the injection timing for MBT, where engine efficiency losses by operating away from MBT were slight. Finally, this effort found that a slight reduction in both Particulate Matter (PM) and NO_x emissions for injection slightly after MBT could be achieved, without sacrificing significant fuel efficiency [10]. While Mattson et al.'s efforts were for ULSD, the performance and emissions findings with changing injection timing should be similar for a biodiesel fuel. Therefore, this work follows-up the previous effort by allowing for variable injection pressures. Specific changes to profile and duration are left to future students. Of note, these items will change dynamically with injection pressure due to more fuel leaving the injector quicker; however, no specific modifications were made to these components during operation.

In regards to adjusting the injection pressure, Hariprasad suggested that for studies employing palm oil methyl ester (POME) and ULSD as a pilot fuel in a dual fueled engine (Liquefied Petroleum Gas - LPG as main fuel), increasing the injection pressure decreases the particle diameter leading to quicker vaporization [67]. However, this decreases the inertia of the fuel affecting its penetration distance in the combustion chamber. As a result, lower CO, HC, and NO_x emissions and higher brake thermal

efficiency (BTE) are observed for POME at increased injection pressure (190-230 bar), and for ULSD at an injection pressure of 210 bar when used as a pilot fuel in operation with LPG under dual fuel operation. Meanwhile, Yuko Mito et al., found that employing higher injection pressures and supercharging leads to a significant reduction of smoke (i.e., PM) emissions for diesel combustion in compression ignition engine [66]. Moreover, employing high levels of Exhaust Gas Recirculation (EGR) in conjunction with POME saw a drop in NO_x emissions without any significant influence on BSFC. As a result, increasing injection and intake pressures resulted in a reduction in the NO_x-PM emissions for a compression ignition engine when EGR is also employed. Donghui et al. suggests that this use of EGR helps offset the usage of higher injection pressures [65]. In specific, higher fuel injection pressures were found to raise NO_x emissions because of improved atomization and better fuel mixture preparation, leading to further decrease in ignition delay. When combined with the relatively high Cetane number of biodiesel, this result in an increase in constant volume combustion, and subsequently higher in-cylinder temperatures; whereas, CO and HC emissions decrease. Employing EGR can lead to a decrease in NO_x emissions through reducing the thermal NO mechanism without causing a significant increase in CO and HC emissions for both diesel and biodiesel fuels. Of note, for this effort EGR will not be utilized, and so the only recycled exhaust gases present will be those that remain in the cylinder after the exhaust stroke is completed.

Pandian et al. found that increasing the injection pressure for a pongamia biodiesel fuel leads to increased brake thermal efficiency (BTE) with lower BSFC at all injection timings [61]. Moreover, a noticeable decrease in CO, HC, and smoke emissions and increase in NO_x emissions were observed. This was because employing higher

injection pressures leads to better atomization of fuel, improved fuel mixture quality, and decreased ignition delay resulting in relatively more constant volume combustion. This leads to relatively higher in-cylinder temperatures and improved combustion efficiency. Furthermore, they suggest that a moderate extended protrusion of nozzle tip (i.e., extending fuel injection penetration length) while increasing the injection pressure resulted in relatively lower BSFC, CO, HC, and NO_x emissions of the fuel.

Other work by Jaichandar et al. studied a combined impact of injection pressure and combustion chamber geometry on the performance of a biodiesel fueled engine [64]. Having a higher injection pressure resulted in a lower BSFC and higher BTE because it results in relatively better atomization of fuel and improved air fuel mixing due to enhanced turbulence of air in the modified combustion chamber design. In addition, they observed a decrease in CO, HC, and smoke emissions; whereas, NO_x emissions grew. Furthermore, the ignition delay of their biodiesel blend fuel was relatively lower for their modified engine with a higher injection pressure as compared to the base engine. The emission results were because of improved atomization and air-fuel mixture quality resulting in shorter ignition delay, improved combustion efficiency, and growth of in-cylinder temperatures.

Similar efforts by Gemus et al. investigated the influence of higher fuel injection pressures on biodiesel and its blends [63]. They suggest that at higher fuel blends (>B10), BSFC decreased with increased injection pressures because the improved atomization of fuel blends negated biodiesel's relatively high viscosity effects. However, BSFC increased for diesel and lower fuel blends (B5) irrespective of injection pressures because the changes in fuel physical properties are negligible when smaller amounts of biodiesel

are in the blend. In general, a greater injection pressure for biodiesel blends leads to a decrease in CO, HC, and smoke emissions while carbon dioxide (CO_2), oxygen (O_2), and NO_x emissions all grew. This is because of improved combustion efficiency due to better atomization of fuel blends leading to enhanced air-fuel mixture preparation and increased pre-mixed burn. This subsequently leads to higher in-cylinder temperatures and with biodiesel being an oxygenated fuel it creates ideal conditions for formation of NO_x, CO_2, and O_2 emissions [60, 62, 63].

Analogous to this effort, Hwang et al. studied the impacts of injection parameters on the combustion and emission characteristics in a common-rail direct injection compression ignition engine fueled with WCO biodiesel [1]. Greater injection pressures at higher loads results in an increase in peak in-cylinder pressures because a larger quantity of fuel is being prepared for auto-ignition. This results in an increase in constant volume combustion and subsequently greater in-cylinder temperatures. This leads to higher NO_x emissions, and a decrease in CO, HC, and smoke emissions since an increase in pre-mixed burn leads to a decrease in diffusion burn resulting in improved combustion efficiency. Kannan et al. concludes the literature findings by illustrating that a higher injection pressure for WCO biodiesel results in an increase in BTE; however, they find a reduction in NO_x emissions along with smoke emissions in contrast to the other researchers [3].

4.3 Literature Consensus

Therefore, from the literature review, one could expect that a higher injection pressure (irrespective of fuel studied) improves atomization of fuel and air-fuel mixture quality. This will lead to a decrease in ignition delay that would act to reduce the amount

of constant volume combustion. However, more of the constant volume type of combustion is actually seen as the mass of fuel injected per unit time increases subsequently resulting in an increase in peak in-cylinder pressures, rate of heat release, and in-cylinder temperatures. Since biodiesel is an oxygenated fuel, an increase in in-cylinder temperatures leads to greater NO_x emissions while CO, HC, and PM emissions decrease. Furthermore, the BSFC is observed to be relatively lower and BTE is observed to be relatively higher due to more constant volume combustion and its enhancement of combustion efficiency.

In order to better understanding these findings, and since there are limited studies with respect to higher injection pressures for a WCO biodiesel fuel in a compression ignition engine, this effort investigates the effects of injection pressure on this fuel in a single cylinder compression ignition test cell. Timing will be adjusted accordingly in order to ensure that the crank angle of peak pressure remains constant during all tests. Moreover, a limit is placed on increasing the injection pressure so that the combustion pressure does not exceed ULSD. Hence, one goal is to mimic the pressure profile of ULSD helping to further normalize combustion between these two fuels. The WCO biodiesel is blended with common Ultra Low Sulfur Diesel (ULSD) in ratios of 5%, 10%, 20%, 50%, and 100% by volume. The WCO biodiesel is supplied by the KU Biodiesel Initiative (KUBI) pilot plant using WCO from the KU dining centers as feedstock material. In the following sections, the experimental setup and methodology, fuel physical properties, in-cylinder pressure traces, rate of heat release, BSFC, and brake specific emissions (CO, CO_2, HC, NO_x, and PM) of WCO biodiesel blends are discussed

in detail with respect to the changes in injection parameters and fuel physical properties from that of ULSD.

4.4 Experimental Setup

For brevity, only major instrumentation highlights will be presented here as Langness et al. provides thorough documentation of the experimental setup along with the specific hardware employed [4]. The test engine is a Yanmar L100V single-cylinder direct-injection CI engine with the stock mechanical fuel injection replaced with a common-rail electronic fuel injection system controlled by a Bosch MS15.1 Diesel Electronic Control Unit (ECU) running Bosch ModasSport. This allows for variable injection timings with resolution of 0.02 degrees per crank angle, and up to five injections per thermodynamic cycle, while allowing for modulation of the injection pressures from 40 to 200 MPa (50.0 ± 0.5 MPa baseline pressure used for this study). An alternating current (AC) air-cooled regenerative dynamometer from Dyne Systems, Inc. acts to modulate the speed of the engine with load adjusted through the fuel injection amount. Torque is measured using a FUTEK transducer (Model #TRS-705) that is installed using couplings between the Yanmar engine output shaft and dynamometer input shaft. A Merriam laminar flow element (Model #50MW20-2) and an Omega differential pressure transducer (Model #PX277-30D5V) are used to measure inlet air mass flow. Fuel flow rate is characterized using a Micro-Motion Coriolis flow meter (Model #CMF010M). A Kistler (Model #6052c) pressure transducer is used to measure in-cylinder pressures and the corresponding crank angle is measured using a Kistler (Model #2614B) encoder. The stock EGR system for the Yanmar engine has been disabled, in favor of an external EGR system that is not utilized here. To characterize emissions in the exhaust stream, an AVL

SESAM Fourier Transform Infrared Spectroscopy (FTIR) emission analyzer is employed. This device measures total hydrocarbons (THCs), CO, and NO_x emissions, among others. Oxygen is measured using a Magnos 106 oxygen sensor. Finally, Particulate Matter (PM) emissions are monitored using an AVL (Model #415S) Variable Sampling Smoke Meter.

The injection timing (standard) of the engine is calibrated to MBT for ULSD such that the minimum amount of fuel is consumed at a particular load setting. In the experimental data that follows, two sets of data are illustrated. ULSD is first tested each day to obtain reference pressure traces for a load sweep (0/25/50/75/100% of rated) ranging from 0.5 N-m to 18 N-m. Note that a positive torque value is employed for 0% engine load to ensure combustion stability. Data collection occurs at a speed of 1800 RPM that represents a mid-point in the operation range of the Yanmar and because of the applicability of the results. Specifically, low-load conditions produce combustion that is primarily premixed (0.5, 4.5, and 9.0 N-m) while higher loads (13.5 and 18.0 N-m) produce combustion that is dominated by diffusion burn. Following the ULSD test, WCO biodiesel blends are first tested at this standard injection timing and pressure at a particular load setting to compare its ignition delay with that of ULSD. Then, the authors normalized the injection timing of the test fuel to match the peak in-cylinder pressure trace crank angle location of ULSD at the corresponding load setting. This is done to compare the effects of fuel properties on combustion while removing the influence of ignition timing that can skew results (e.g., earlier combustion can lead to higher NO_x emissions through the thermal NO effect). Now, the fuel injection pressure is steadily increased to match peak in-cylinder pressure of ULSD (if possible) at a particular load setting (with timing adjusted if needed). The data is collected only after achieving steady-

state for all the cases. Steady-state is determined based on changes in downstream exhaust gas temperatures; a change less than 1% in one minute is considered steady-state. This process is repeated for the entire load sweep. The in-cylinder pressure data taken for 60 thermodynamic cycles after steady state is reached and averaged pressure data with standard deviation is presented to analyze performance characteristics. In addition, emission data is taken for a period of five minutes after steady state is reached with one reading per second amounting to a total of 300 readings which are averaged with standard deviation is presented to analyze emission characteristics. Between tests, the fuel system is bled and flushed with the new fuel blend, subsequently running for about 30 minutes to ensure that no old fuel remains in the system. During this time, in-cylinder pressure traces are observed for changes in ignition delay indicating combustion of the new fuel blend. Upon completion of testing, the raw data is post-processed in order to obtain averages and uncertainties.

4.5 Fuel Analysis

In order to diagnose the influence of fuel properties on combustion, the ASTM laboratory on campus was employed in order to measure the properties of neat WCO biodiesel and ULSD presented in Table 1. The specific equipment employed in determining this information includes a Koehler KV4000 Series Digital Constant Temperature Kinematic Viscosity Bath KV4000 (ASTM D445), 6200 PAAR Calorimeter (ASTM D240), Anton Paar 5000 M DMA Density meter (ASTM D4052), and Optidist distillation unit (ASTM D86). The Cetane Number is obtained based on a calculated measurement based on data obtained from density and distillation tests. While the properties of the fuel blends are estimated based on the method used by Ertan et al. [69].

Table 16. Characteristics of the WCO biodiesel and ULSD [3, 5, 6, 69]

Property	ULSD	W5	W10	W20	W50	W100
Density (kg/m^3)	841.00 ± 0.01	*843.15*	*844.99*	*848.66*	*859.66*	878.00 ± 0.01
Kinematic Viscosity (cSt)	2.74 ± 0.0044	*2.74*	*2.75*	*2.85*	*3.39*	4.61 ± 0.0048
Dynamic Viscosity (cP)	2.31	*2.31*	*2.32*	*2.42*	*2.91*	4.05
Cetane Number (CN)	48.61	*48.82*	*49.03*	*49.45*	*50.71*	52.80
Energy Content (kJ/kg)	45670 ± 47	*45197*	*44724*	*43778*	*40940*	36210 ± 47
Energy Content (MJ/m^3)	38423 ± 40	*38108*	*37791*	*37153*	*35194*	31792 ± 41.62

The fuel injection system implemented is a high-pressure rail direct injection system that is controlled by an ECU, resulting in highly accurate control of fuel injection timing and amount. It adds fuel on a volumetric basis; hence, the inclusion of the calculated MJ/m^3 row in Table 16. The ASTM laboratory data indicates that the lower energy content and higher density of WCO biodiesel leads to a relatively lower volumetric energy content in comparison to ULSD. This suggests that employing the same fuel injection pressure will result in a less immediate energetic combustion event. However, as fuel injection pressure increases and the fuel flow rate per unit time increases, it is possible that more energy could be added via WCO biodiesel in comparison to ULSD.

Furthermore, the higher viscosity of WCO biodiesel indicates that it is relatively more difficult to atomize the fuel leading to a reduced mixing of the fuel and air. This again suggests a lower relative release of energy from the fuel. Nevertheless, with increasing injection pressure, fuel atomization is generally improved, leading to better

air-fuel mixture preparation. The ASTM Cetane number tests suggest that WCO biodiesel blends will ignite more readily than ULSD. This leads to a reduced (less energetic) pre-mixed combustion phase, because less time is needed before ignition occurs; hence, less fuel is capable of being prepared during the ignition delay period. This would result in relatively lower peak in-cylinder pressures, temperatures, and oxides of nitrogen (NO_x) emissions. As fuel injection pressure increases, it is possible that the pre-mixed combustion phase of WCO biodiesel might actually increase over ULSD resulting in higher NO_x emissions. This would result in reduced diffusion burn combustion and lower PM emissions. A detailed study on combustion analysis of biodiesels by blend percentage was performed in a previous study at standard injection pressures over the entire load range and, as a result, the focus here is largely regarding the influence of injection pressure instead of blend percentage [70].

4.6 Results

4.6.1 In-Cylinder Pressure Traces

In Figure 18, the influence of fuel injection pressure on in-cylinder pressures of WCO biodiesel blends are presented with respect to crank angle for the entire load range. Of note, in the graphs that follow the nomenclature is presented as WX_Y where X is the percentage of biodiesel by volume in the fuel and Y is the injection pressure employed for that particular fuel blend and load. The fuel injection pressure is increased from the standard injection pressure for ULSD at a particular load setting (i.e., 50.0 MPa) until (1) the effects are not seen in the results, or (2) the peak pressure of biodiesel blend matches that of ULSD. Of note, multiple injection pressure results are provided to help illustrate its effect.

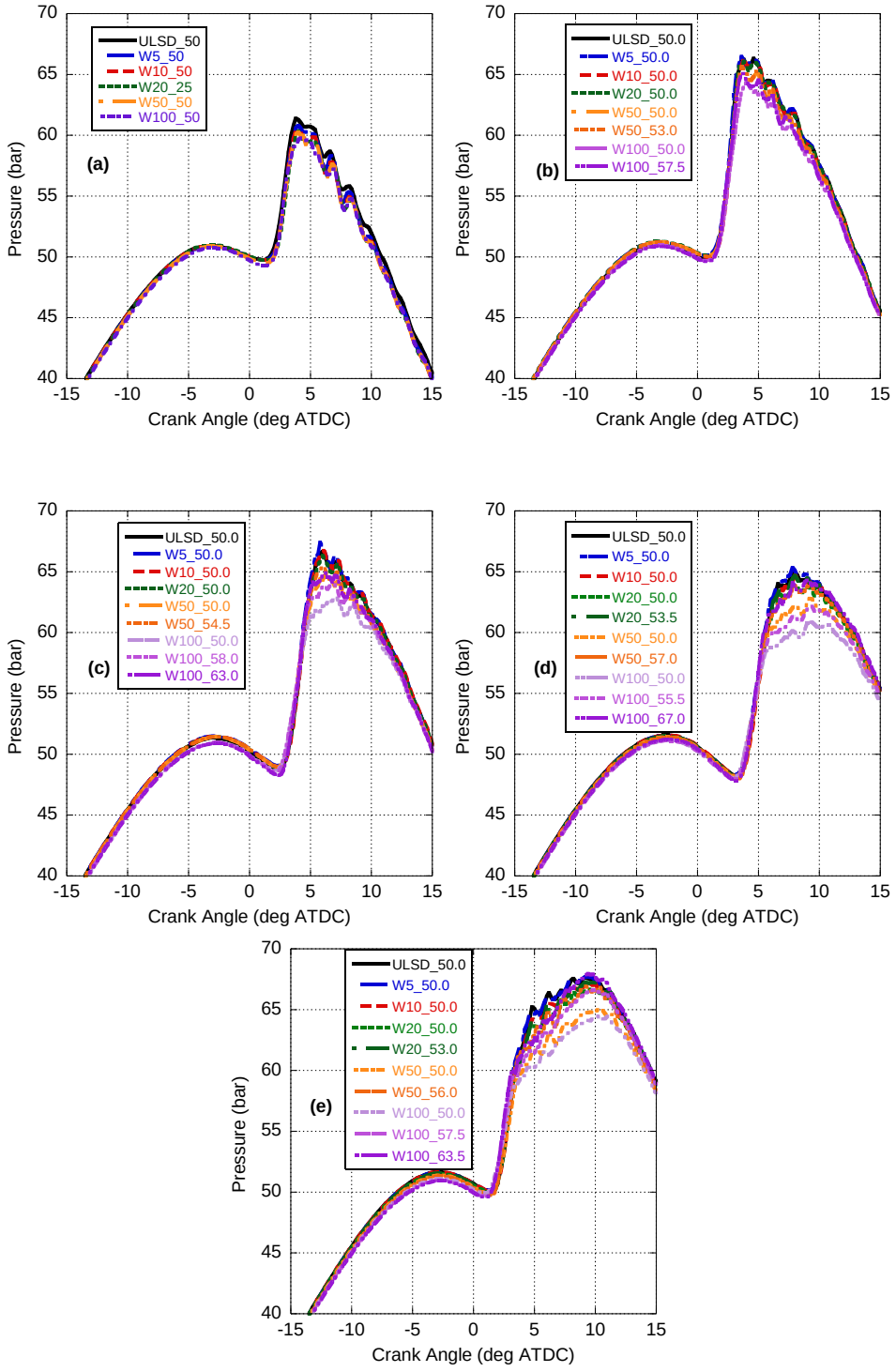

Figure 18. In-cylinder pressure traces with respect to crank angle for 0% (a), 25% (b), 50% (c), 75% (d), and 100% (e) load as a function of WCO biodiesel volume percentage

At lower WCO biodiesel blends (5% and 10%), irrespective of the load, changing the injection pressure had a negligible influence on in-cylinder pressure traces. Investigating the blend properties in Table 16, one finds that there is negligible change in fuel physical properties at these blends compared to ULSD. Recently submitted work by Mattson et al. found that for palm biodiesel blends, the changes in combustion for 5% and 10% fuel blends are negligible in comparison to ULSD, as shown through a heat release analysis utilizing either the 1st or 2nd law of thermodynamics [71, 72]. Overall, it is to be expected that low-percentage blends of any biodiesel with ULSD would have similar fuel qualities as the ULSD fuel properties vastly outweigh those of the biodiesel fuel, and thus similar combustion processes. Hence, changing the injection pressure for these fuels should not noticeably influence the results.

At low to mid loads (0.5 to 9.0 N-m), combustion is primarily pre-mixed with little to no diffusion burn. Hence, nearly all fuel will enter prior to combustion happening, as the ignition delay is long enough to allow for complete fuel injection, proper atomization, vaporization, and mixing. Moreover, as Mattson et al. showed, 20% biodiesel blend deviation from ULSD was significant (if small), and was directly linked to the larger changes in fuel chemistry for blends of around 20% biodiesel content above 9.0 N-m load, although this result was only apparent when using a 2nd law heat release analysis instead of the traditional 1st law model [72]. Therefore, changing the fuel injection pressures for blends of 20% or less had no significant impact on pressure trace at these loads.

However, for high blends of WCO biodiesel, the fuel properties start to influence the relative amount of pre-mixed burn beyond 0.5 N-m. This is because changes in

viscosity and Cetane number of the fuel blends are significant as shown in Table 16. The influence of changing fuel physical properties is made evident by the decrease in pre-mixed burn and increase in diffusion burn regions due to poorer atomization and air-fuel mixture preparation at standard fuel injection pressures, which become more significant as biodiesel content increases. Employing higher injection pressures results in improved atomization and air-fuel mixture preparation at higher fuel blends above the 0.5 N-m load setting, as the effects of viscosity are offset through enhanced mixing.

At high loads, the greater level of diffusion burn starts significantly influencing the in-cylinder pressure trace. This is where the 20% blend starts to noticeably deviate from ULSD at the same injection pressure (similar to Mattson et al.'s findings using both 1^{st} and 2^{nd} law heat release models), and injection pressure must be increased in order to match ULSD peak pressure. Furthermore, substantial changes to injection pressure are required for 50% and 100% blends in order to account for their relatively large changes in fuel properties. Hence, from an ECU and in-cylinder pressure standpoint, it appears that 5% and 10% biodiesel blends can be used as-is with minimal adjustments to engine operation. Whereas, 20% blends require only slightly higher injection pressures when it become important to mitigate diffusion burn (i.e., at higher engine loads), and 50% to 100% blends nearly always require dramatic changes to injection pressure to match ULSD peak pressure for all engine loads. As mentioned prior, while employing higher injection pressures, injection timing was adjusted accordingly to match the peak pressure crank angle location of ULSD to remove any influence of drop in ignition delay on performance of test fuel.

Of note, the changes to injection pressure and subsequently the injection timing to maintain peak pressure crank angle location are presented in Table 17. As indicated, there was a small adjustment to 10% biodiesel blend injection timing given the high fidelity of the single-cylinder pressure trace measurement; however, it is anticipated no significant adjustment is needed for a multi-cylinder engine as crankshaft loads are more equally balanced across multiple cylinders. Therefore, based on the in-cylinder pressure results and the literature survey, 5% and 10% blends used as-is will demonstrate no significant difference in contrast to ULSD at the same injection timings and pressures.

Table 17. Normalized injection timings and optimum injection pressures of WCO biodiesel blends and ULSD across the entire load range

Torque (N-m)	ULSD		W5		W10		W20		W50		W100	
	bTDC	MPa	bTDC	MPa	bTDC	MPa	bTDC	MPa	bTDC	MPa	bTDC	MPa
0.5	12.5	50.0	12.5	50.0	12.3	50.0	12.1	50.0	11.9	50.0	11.7	50.0
4.5	12.5	50.0	12.5	50.0	12.3	50.0	12.2	50.0	11.9	53.0	11.6	57.5
9.0	11.0	50.0	11.0	50.0	10.8	50.0	10.7	50.0	10.5	55.0	10.0	63.0
13.5	10.0	50.0	10.0	50.0	9.8	50.0	9.6	53.5	9.3	57.0	8.9	67.0
18.0	11.0	50.0	11.0	50.0	10.8	50.0	10.6	53.5	10.4	56.0	10.5	57.5

4.6.2 Rate of Heat Release

Computing the heat release rate of the fuel blends helps to further illustrate the influence of WCO biodiesel fuel properties upon combustion. The rate of heat release at each crank angle is calculated as shown in Figure 19 using a model based on a chemical equilibrium for estimation of cylinder contents satisfying the first law of thermodynamics [71]. Following along the same lines as the in-cylinder pressure discussion, for 5% and 10% blends, the peak rate of heat release is observed to be similar to that of ULSD due to

negligible influence of change in fuel physical properties. Thus, there was no need to employ higher injection pressures to optimize the combustion of these fuel blends.

From low to mid range loads (0.5 to 9.0 N-m), combustion is observed to consists largely of only pre-mixed burn as shown in Figure 19. This is because fuel injection, atomization, vaporization, and air-fuel mixture preparation of most of the injected fuel is completed within the ignition delay at corresponding injection pressures of fuel blends. For the 20% fuel blend, no noticeable deviation in performance is observed up until 9.0 N-m; thus, standard injection pressures are employed prior to this point. At higher loads beyond 9.0 N-m, a slight deviation in the performance of fuel blend is seen because of the relative change in fuel properties increase as found by Mattson et al. [72]. This leads to a small drop in pre-mixed burn region followed by slight increase in diffusion burn above the 9.0 N-m load setting. Thus, slightly higher injection pressures are applied to optimize combustion of this fuel blend at higher loads as shown in Figure 19.

For higher blends above 20%, a significant change in fuel physical properties influences the performance of WCO biodiesel blends above the 0.5 N-m load setting. Thus, higher injection pressures are employed to optimize the combustion of WCO biodiesel blends to attempt to replicate the performance of ULSD. Furthermore, increasing the injection pressure results in a growth of the pre-mixed burn spike while the diffusion burn phase decreases. This helps to negate the influence of higher viscosity of fuel blends on combustion as shown in Figure 19.

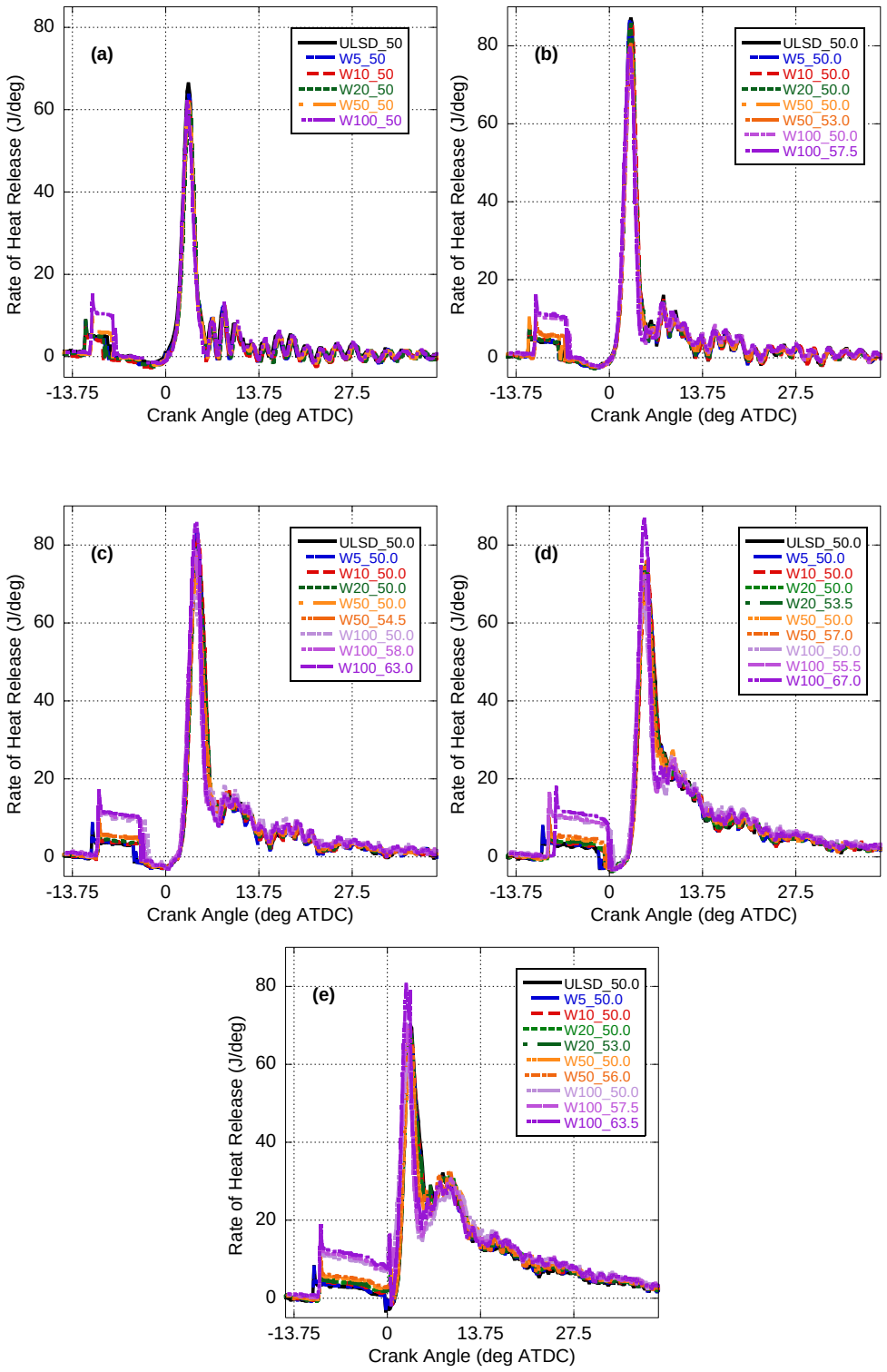

Figure 19. Heat release rates with respect to crank angle for 0% (a), 25% (b), 50% (c), 75% (d), and 100% (e) load as a function of WCO biodiesel volume percentage at normalized injection timings

4.6.3 Brake Specific Fuel Consumption

Of note, the rate of heat release during the fuel injection period is positive in Figure 19 as opposed to being negative due to the loss of heat from cylinder gases because of fuel vaporization. This anomaly is due to an assumption in the heat release model that injected fuel is instantaneously atomized and vaporized; thus, adding energy to the gas from the liquid fuel model. While erroneous, this is helpful in the diagnosis of the BSFC in Figure 20. In specific, the overall length of injection between ULSD and WCO biodiesel blends does differ noticeably and BSFC values are relatively higher for higher blends of WCO biodiesel at standard injection pressures as shown in Table 18. This is because the energy content per mass of WCO biodiesel is lower and the atomization process is worse due to a higher viscosity, resulting in need for more total mass in order to achieve same torque and peak rate of heat release as that of ULSD.

When increasing the injection pressure had a noticeable influence on in-cylinder results, the BSFC of WCO biodiesel improves as shown in Table 18. In other words, the reduction in constant volume combustion and thermal efficiency through a relatively high viscosity and lower volumetric energy content of WCO biodiesel at standard fuel injection pressure is overcome by improving the fuel mixture preparation while increasing the mass of fuel entering by employing higher fuel injection pressures. Hence, there is a greater amount of mixture prepared during the pre-mixed (aka constant-volume) phase of combustion. However, the BSFC of higher fuel blends is still observed to be relatively higher as compared to ULSD due their lower energy content by mass and volume as illustrated in Figure 20. Of note, at certain loads and fuel blends no change in

BSFC is observed since higher injection pressures were not necessary for optimal performance of fuel.

Table 18. Comparison of Brake Specific Fuel Consumption (g/kW-hr) between standard and higher pressure injections

Load N-m	ULSD	W5	W10	W20	W20_hp	W50	W50_hp	W100	W100_hp
0.5	2242.32	1955.38	2274.1	3065.84	3065.84	2259.42	2259.42	2335.94	2335.94
4.5	413.77	399.52	406.03	403.39	403.39	425.62	421.84	463.38	453.24
9.0	280.8	283.35	284.66	288.91	288.91	301.11	301.07	323.93	323.53
13.5	246.18	248.78	250.66	254.66	252.67	264.77	262.88	284.08	281.99
18.0	234.09	235.99	238.01	242.32	241.09	252.91	252.26	273.79	271.56

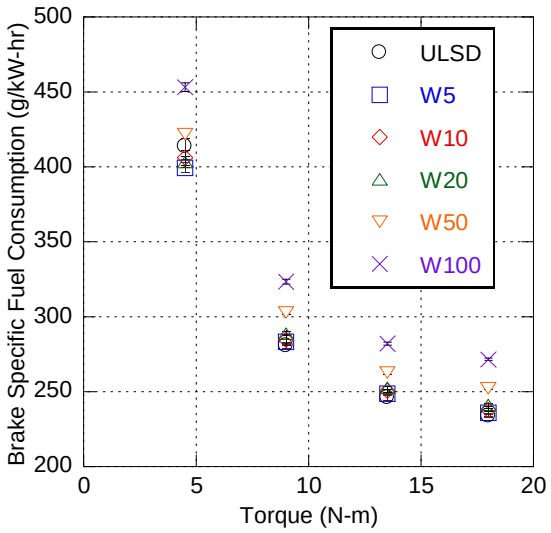

Figure 20. Brake specific fuel consumption vs. engine torque for normalized injection timing and optimum high injection pressures (note: error bars are included)

4.6.4 In-Cylinder Temperature Traces

To further investigate the combustion process and analyze brake specific emissions, in-cylinder temperature is employed as calculated from the measured pressure data via the heat release model. Since the injection timing is adjusted by peak pressure location, the peak temperatures do not necessarily align between ULSD and WCO

biodiesel blends. In addition, the initial temperature before combustion begins (i.e., compression temperatures) may differ due to the relative amount of heat transfer and exhaust gas temperatures. For example, a hotter in-cylinder combustion process will promote more heat transfer to the walls raising the gas temperature during the following compression process. Moreover, a hotter exhaust gas will result in a warmer in-cylinder residual, increasing the initial charge temperature. This is evident in Figure 21(e) for high WCO biodiesel blends; peak temperature is higher resulting in a hotter compression temperatures.

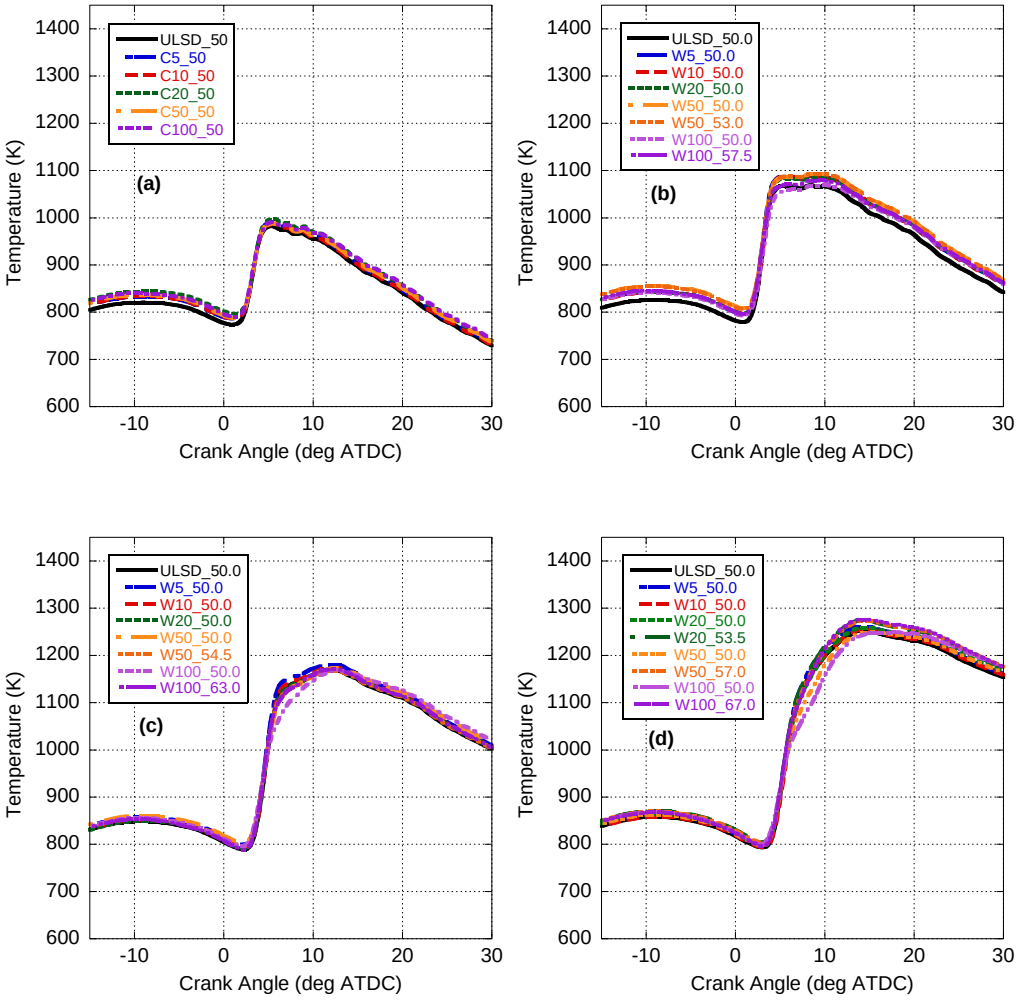

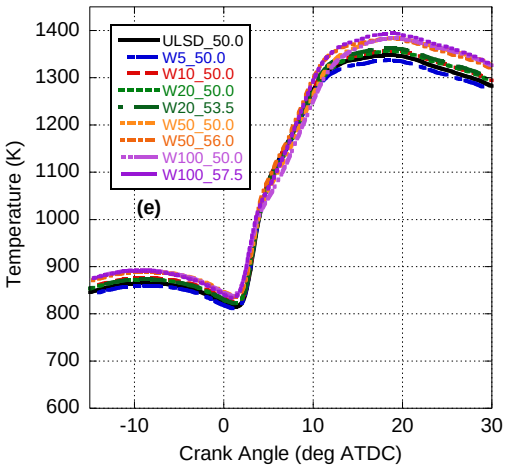

Figure 21. Cylinder temperature vs. engine crank angle at 0.5 N-m (a), 4.5 N-m (b), 9.0 N-m (c), 13.5 N-m (d), and 18.0 N-m (e) at optimal injection pressures

Before discussing the temperature trends, three previous items are re-iterated:

1. Below 20% fuel blend, the combustion is observed to be similar to that of ULSD due to negligible changes in fuel properties.
2. Employing higher injection pressures resulted in an increase in pre-mixed heat release spike.
3. The brake specific fuel consumption values are relatively greater for WCO biodiesel fuel blends; indicating more fuel is required to obtain similar performance as that of ULSD at a particular load setting.

From this information, it is anticipated that the maximum temperature below 20% fuel blend across the load range should be similar to that of ULSD (item #1). Furthermore, the increase in pre-mixed spike with an increase in injection pressure suggests a growth of constant volume combustion and a subsequent hotter burn (item #2). In addition, higher peak temperatures occur for WCO biodiesel blends as the relative amount of fuel burnt increases promoting a more exothermic combustion process; albeit

shifted towards the diffusion burn phase (item #3). This is what is largely seen in Figure 21 with a few outliers. In specific, WCO biodiesel blend maximum temperature is similar to ULSD at 5% and 10% blend, slightly higher at 20% blend, and significantly higher at 50% and 100% blends while also increasing in magnitude with greater fuel injection pressures (while shifting slightly to the right through diffusion burn combustion).

4.6.5 Brake Specific Emissions

The performance analysis is used in conjunction with fuel physical properties to analyze brake specific emissions at all loads and injection strategies. Emissions presented as a function of engine brake torque are called brake specific emissions. The brake specific emissions of oxides of nitrogen (NO_x), carbon monoxide (CO), total hydrocarbons (THC), and particulate matter (PM) are shown as a function of engine torque at normalized injection timings and optimum injection pressures in the following sections. There is observed to be higher variability at 0.5 N-m loading due to normal cyclic variation in engine operation causing higher measurement uncertainty at such a low engine load.

Brake Specific NO_x Emissions

The brake specific NO_x emission results in Figure 22 are composed of a collection of nitric oxide (NO) and nitrogen dioxide (NO_2). The data presented here for a WCO biodiesel blend uses the optimized injection pressure for a particular fuel blend and corresponding load setting, as discussed previously. These NO_x compounds are typically formed in fuel-lean and high temperature zones of combustion, typically on the periphery of the injected fuel spray. A previous effort employing this engine compared neat biodiesels and ULSD at equivalent injection pressures and found an increase in in-

cylinder temperatures due to a greater diffusion burn energy release also resulting in hotter residual gases (i.e., less efficient expansion process). Moreover, biodiesel was stated to have a higher adiabatic flame temperature contributing to larger in-cylinder temperatures. Furthermore, it was found that the oxygen content in the biodiesel lowers the respective equivalence ratio of fuel mixture making the overall global value nearly equivalent to ULSD (even though more fuel was added), subsequently removing its relative influence on NO_x emission formation. As a result, NO_x emissions were found to be lower for neat biodiesel fuels largely because the amount of pre-mixed combustion decreased (early stage NO_x formation) even though hotter global temperatures were found [58]. Hence, with increasing blend percentage, one could anticipate a reduction in NO_x emissions if the injection pressure was held constant.

In this effort, when the standard injection pressure was observed to be sufficient for optimum combustion of blend, the NO_x results follow the prior paper discussion. However, once the blend required higher injection pressures to mimic ULSD, most notably at 50% and 100% WCO biodiesel, NO_x emissions began to increase over the ULSD baseline. Even though the BSFC improved with injection pressure (i.e., less energy potential), its relative decrease did not outweigh the growth in early NO_x formation through a greater pre-mixed burn phase. Hence, there are two factors playing a significant role with increased injection pressure; (1) a greater pre-mixed combustion phase leads to higher temperatures (over and above the prior paper) and (2) more early combustion gives additional time for NO_x kinetics. These factors are the catalyst for exponential growth of NO_x emissions reversing the previous paper trend with biodiesel.

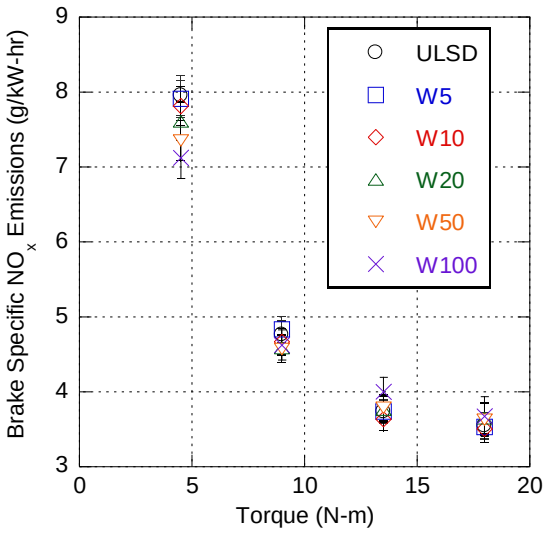

Figure 22. Brake Specific NO_x emissions vs. engine torque for normalized injection timing and optimum injection pressures

Brake Specific CO and THC Emissions

The emissions of CO and THC are primarily formed due to inefficient combustion, but CO may also be traced to the dissociation of CO_2 in the high temperature environment. At standard fuel injection pressures as that of ULSD, the WCO biodiesel blends are expected to have lower combustion efficiencies, due to poorer atomization and vaporization as compared to ULSD. This leads to the anticipation of higher brake specific CO and HC emissions for WCO biodiesel blends. However, the oxygen content and lower carbon ratio of WCO biodiesel promotes the oxidation of CO and THC, resulting in lower brake specific CO and THC emissions with increase in biodiesel content in the fuel blend. With respect to temperature, the globally hotter combustion environment with biodiesel blend promotes CO_2 dissociation and better combustion efficiencies. Overall, the CO and HC emissions for WCO biodiesel blends are expected to be lower as compared to ULSD due primarily to the oxygen in the fuel and approach close to that of

ULSD as the load increases at standard injection pressures when the amount of fuel added dramatically grows.

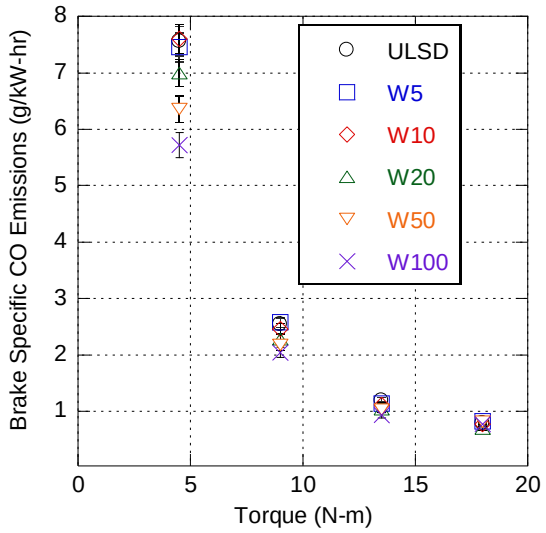

Figure 23. Brake specific CO emissions vs. engine torque for normalized injection timings and optimum injection pressures

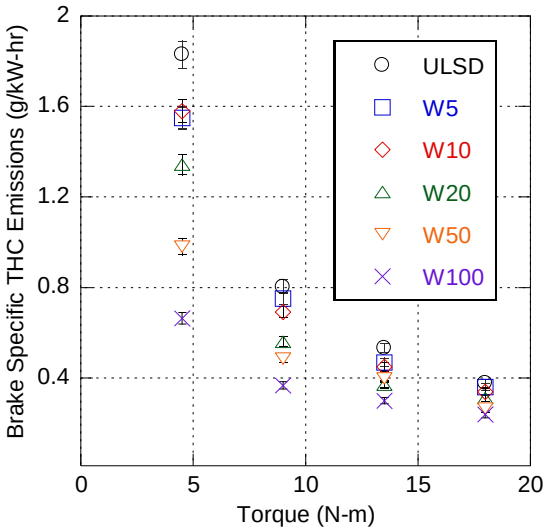

Figure 24. Brake specific THC emissions vs. engine torque for normalized injection timings and optimum injection pressures

As a result, for this effort when the injection pressure had a negligible influence on the results, CO and THC emissions were found to be lower. Moreover, increasing the

injection pressure led to a hotter and earlier burn, subsequently promoting better combustion efficiencies and lower CO and THC emissions. This is buffered somewhat by enhanced CO_2 dissociation. However, the high oxygen content of WCO biodiesel blends promotes the oxidation of CO to CO_2 that slightly offsets this CO_2 dissociation factor. Furthermore, since BSFC decreases with injection pressure, less carbon and hydrogen is added subsequently lowering CO and THC emissions. Overall, less CO and THC emissions of WCO biodiesel blends are seen at lower loads and approach to that of ULSD as the load increases for higher WCO biodiesel blends (albeit less than when maintaining the injection pressure), as shown in Figure 23 and Figure 24, respectively.

Brake Specific PM Emissions

Particulate Matter (PM) emissions are typically formed when combustion happens around a fuel-rich core. The WCO biodiesel blends are generally believed to have higher amounts of brake specific PM emissions below full load condition at standard fuel injection pressures than that of ULSD, due to poorer atomization and mixture preparation, resulting in greater levels of diffusion-controlled combustion. At full load, previous efforts found relatively higher brake specific PM emissions for ULSD as compared to neat biodiesel fuels since enough oxygen from the biodiesel now sufficiently leans out the rich fuel cores [58].

In this study, when the injection pressure remained constant between ULSD and biodiesel blend, generally the biodiesel blend had higher PM emissions due to the mechanisms presented in [58]. However, in those scenarios when fuel injection pressure had an influence on the results, PM emissions for biodiesel blends decreased below that of ULSD as shown in Figure 25. Hence, at 13.5 N-m the trend from the earlier paper was

reversed and biodiesel blends were now lower. This can be traced back to the increase in the pre-mixed burn phase and subsequent decrease in diffusion burn phase as fuel injection pressure increases. This change is more dramatic after 9.0 N-m when combustion starts to be largely controlled by diffusion burn. Overall, as one would expect from the NO_x-PM tradeoff, as NO_x emissions increase because of a greater amount of pre-mixed burn, PM emissions will decrease.

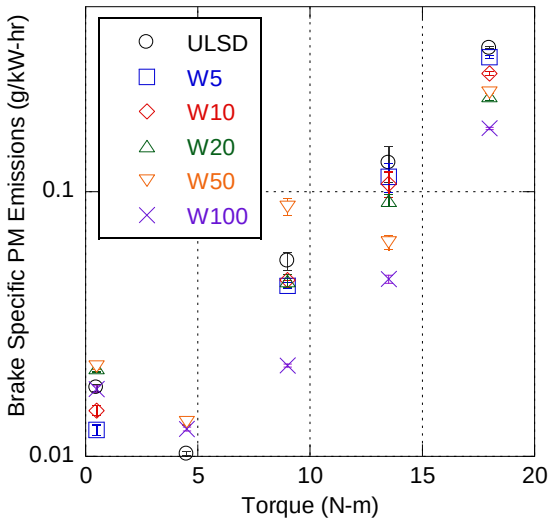

Figure 25. Brake specific PM emissions vs. engine torque for normalized injection timing and optimum injection pressures

4.6.6 Comparison of LCA of the Test Fuels

The emissions produced during the LCA of WCO biodiesel are updated with data obtained from PtE analysis of WCO biodiesel at optimum injection pressures during this study. In addition, this data is compared with emissions produced during WtE analysis of WCO biodiesel and WPF from the previous chapter to study the influence of higher injection pressures on emissions produced during LCA of these fuels from cradle to grave as shown in Table 19.

Table 19. Comparison of emissions produced (g/kg_{fuel}) from WtE analysis of test fuels at full load (18.0 N-m)

WtE	ULSD	WPF	WCO Biodiesel	WCO Biodiesel (optimization)
VOC	0.578	0.522	0.526	0.509
CO	6.114	5.788	4.361	3.640
NO_x	19.903	19.247	13.620	15.115
PM	2.348	2.705	1.762	1.468
SO_x	0.897	0.219	0.382	0.384
CH_4	5.706	1.080	2.047	2.044
N_2O	0.042	0.038	0.029	0.029
CO_2	2746.304	2795.409	2039.865	2057.263

The emissions produced during the WtE analysis of WCO biodiesel at higher injection pressures suggests that the relatively lower VOC, CO, PM, and CH_4 are due to the improved atomization and enhanced air-fuel mixture preparation. This results in more constant volume combustion improving combustion efficiency. In addition, the increase in NO_x emissions is due to this more energetic pre-mixed burn phase that promotes the thermal NO mechanism. An unexpected finding was the increase in CO_2 emissions. As fuel injection pressure increases, less fuel is burned resulting in less total CO_2. This is counteracted by an increase in CO and THC conversion resulting in more CO_2. Overall, the ratio of added CO_2 to decreased BSFC in Table 19 promotes an increase in CO_2 per kg_{fuel}. Finally, the SO_x and N_2O emissions are observed to be similar irrespective of change in injection pressures.

Based on the above discussion with respect to an improved LCA of WCO biodiesel at higher injection pressures, similar results could be obtained for WPF at higher injection pressures. Employing higher injection pressures for optimal combustion of WPF could potentially lead to relatively lower VOC, CO, PM, and CH_4 emissions due to improved combustion efficiency by negating the high viscosity of the fuel. In addition, NO_x emissions could be anticipated to be higher due to the enhanced pre-mixed burn

phase. However, CO_2 emissions could move in either direction depending on the relative magnitude of CO_2 growth through enhanced combustion and CO_2 mitigation through reduced fuel consumption.

4.7 Conclusion

Biodiesel is a viable alternative to fast-depleting fossil fuels. Biodiesels produced from virgin oils incur significant costs compared to conventional petroleum diesel fuel. Studies have shown that about 78% of conventional biodiesel production costs comes from production of feedstock for synthesis of biodiesel [3]. Usage of waste cooking oil (WCO) as a feedstock material for synthesis of biodiesel has gained significant interest since it not only solves disposal issues of WCO but also lowers the cost of production of biodiesel. The biodiesels are certainly different from commercial diesel with respect to fuel characteristics. As a result, it is necessary to understand the combustion of these fuels in compression ignition engines in order to optimize fuel performance while minimizing emissions by employing higher fuel injection pressures and normalized injection timings to attempt to replicate the performance of ULSD.

This study is performed in order to better understand the influence of injection pressure on the performance and emission characteristics of WCO biodiesel blends with ULSD. The combustion analysis was performed for each fuel blend at five load cases ranging between (0.5 N-m to 18.0 N-m) at consistent load settings with an increase in fuel injection pressures where needed to replicate the in-cylinder pressure of ULSD. At 5% and 10% blends, standard injection pressures were sufficient for optimal injection performance due to a negligible change in fuel properties. For the 20% blend above 9.0 N-m load, the influence of changing fuel properties is observed through its performance

at standard injection pressures, where the increase in viscosity serves to degrade fuel atomization and air-fuel mixture preparation. Thus, higher injection pressures are employed to optimize the combustion in an attempt to replicate the combustion of ULSD. Furthermore, at higher fuel blends above 20% and above 0.5 N-m load, a significant drop in performance of the fuel blends is observed as compared to ULSD at standard injection pressures. Employing higher fuel injection pressures leads to a steady increase in pre-mixed burn region and decrease in diffusion burn region. This leads to an increase in peak in-cylinder pressures, peak rate of heat release, global temperatures, and enhanced combustion efficiencies.

The result is that the brake specific fuel consumption of WCO biodiesel blends is observed to decrease with higher injection pressures via the promotion of constant volume combustion. The brake specific NO_x emissions of WCO biodiesel blends were observed to be slightly lower at lower loads but now surpass ULSD at higher loads illustrating a reversion of prior literature trends. Furthermore, the brake specific CO and THC emissions are observed to be lower because of the improved combustion efficiency due to the employment of higher fuel injection pressures. PM results follow the literature (i.e., higher for blends at low loads, lower at higher loads), but now reverse at a lower load setting.

The comparison of emissions produced during LCA of WCO biodiesel at standard injection pressures and at higher injection pressures suggests lower CO, VOC, PM, and CH_4 emissions and higher NO_x and CO_2 emissions while changes in SO_x and N_2O emissions are negligible. In addition, similar performance is anticipated to be seen with

respect to the LCA, if the combustion of WPF is optimized by increasing the injection pressures.

Chapter V: Conclusion

The combustion performance of waste-derived fuels, derived from plastic solid waste and waste cooking oil, was studied with respect to ultra low sulfur diesel (ULSD) fuel in a single cylinder compression ignition engine test cell. In addition, the life cycle analyses of these fuels were performed with respect to ULSD to compare emissions produced during creation and combustion with normalized functional unit of 36 gallons of output fuel.

Chapter 2 focused on the combustion analysis of waste plastic fuel (Cyndiesel) blends with respect to ULSD in a compression ignition engine test cell at standard injection pressures. The results suggest that the performance and emission characteristics of Cyndiesel at lower (<20%) blends is similar to that of ULSD. Thus, 5% and 10% Cyndiesel fuel blends could be directly used in commercial compression ignition engines without any calibration modifications. At higher Cyndiesel fuel blends, a drop in peak in-cylinder pressures and pre-mixed burn phase was observed with an increase in load. Overall, the brake specific fuel consumption of Cyndiesel fuel blends was found to be similar to that of ULSD due to the higher embedded energy of the fuel. In addition, brake specific NO_x emissions are shown to be lower, while brake specific PM emissions are found to be higher with increasing blend percentage over the entire load range as combustion shifts more towards the diffusion burn phase. Furthermore, the brake specific CO and THC emissions are relatively lower as compared to ULSD in deference to idealized trends. Fuel chemistry is believed to play a significant role in reversion of these

trends. In specific, CHN data in conjunction with literature findings on reduction of unsaturated bonds (C=C) and increase in saturated (C-H) bonds when employing catalytic pyrolysis can potentially explain this result. For operation of higher blends of Cyndiesel in a commercial compression ignition engine, significant modification to the calibration of the engine is required for optimal performance.

Chapter 3 describes and compares life cycle analyses (LCA) of waste-derived fuels with ULSD. These LCAs account for emissions produced during creation and combustion of the respective fuels. All the synthesis techniques are normalized to a functional unit of 36 gallons of output fuel in order to frame the findings in the appropriate comparative light. The LCA in this study was performed from well-to-exhaust (WtE) that is summation of results from well-to-pump (WtP) and pump-to-exhaust (PtE) analysis. The results suggest that the LCA of WCO biodiesel was observed to be relatively lower as compared to waste plastic fuel (WPF) and ULSD. The majority of the emissions in the WtP analysis of test fuels came from the production of electrical energy (here a coal thermal power plant) used in the fabrication pathways. These emissions could be lowered significantly if electrical energy used to power production pathways comes from clean energy sources like wind or solar.

The emissions produced during the WtP analysis could further be improved by employing appropriate modifications to production pathways. For example, residual methanol used in the production of WCO biodiesel could be recycled to reduce methane emissions. Furthermore, the emissions produced during PtE analysis could be improved by employing higher injection pressures to attempt to match the peak in-cylinder

pressures of corresponding ULSD baseline test at normalized injection timing by negating the relatively high viscosities of WCO biodiesel and WPF.

Chapter 4 studied the influence of fuel injection pressure on the performance and emission characteristics of WCO biodiesel fuel blends with ULSD. The injection timing was normalized by matching the crank angle location of peak pressures of ULSD at a particular load setting for any changes in ignition delay with an increase in injection pressure. In addition, the injection pressure was increased in an attempt to match the performance of ULSD for any deviations in performance of WCO blends at standard injection pressures due to the relatively high viscosity of test fuel at a particular load setting. The results of this study suggest that at lower (<20%) blends of WCO biodiesel blends, the standard fuel injection pressures were sufficient to obtain similar performance as that of neat ULSD without any modification with respect to calibration. While at higher fuel blends, a significant drop in performance of fuel blends was observed at standard injection pressures. Thus, higher injection pressures were employed for these blends in an attempt to match the performance of ULSD at a particular load setting by negating the relatively high viscosity of the fuel blends. Employing higher injection pressures leads to improved atomization and enhanced air-fuel mixture preparation while increasing the combustion efficiency, amount of constant volume combustion, and in-cylinder temperatures. Even with an improvement in efficiency, the brake specific fuel consumption was observed to be higher for greater WCO biodiesel fuel blends due to the relatively lower energy content by mass and volume as compared to ULSD. The emission characteristics of this study suggest a reversal of prior biodiesel trends for NO_x emissions with NO_x now increasing over ULSD when injection pressure is optimized. Brake

specific CO and THC emissions are observed to be lower with WCO biodiesel fuel blends due to the increase in combustion efficiency and presence of oxygen in the fuel blends. Furthermore, literature trends are validated with respect to PM emissions being higher at low loads, but reduced at higher loads because of the influence of fuel oxygen. However, the reversion now comes sooner as the increased fuel injection pressure promotes a reduced diffusion burn phase. From the calibration point of view, lower (<20%) blends of WCO biodiesel do not require any changes in the calibration of commercial compression ignition engines. However, for higher WCO biodiesel fuel blends, significant changes to the calibration are required for optimal performance. Similar performance and emission characteristics could be obtained for WPF with an increase in fuel injection pressures.

Future efforts could include an additional fuel chemistry analysis to completely understand the reversion of brake specific CO and THC emissions for WPF blends. In addition, higher fuel injection pressures should be employed in order to improve the atomization of WPF blends due to its higher viscosity than ULSD. This could help mitigate the increased PM emissions while still achieving NO_x emissions below that of neat ULSD. Moreover, additional studies could be performed to study the influence of other injection parameters in combination on the performance and emission characteristics of test fuels. Furthermore, the life cycle analysis of WCO biodiesel could be expanded to production of syngas from the glycerin [46] (a byproduct of WCO biodiesel production). Finally, a pilot plant could be setup for production of waste plastic fuel from PSW collected by KU recycling on campus. In near future, both these fuels

could be used in KU on Wheels buses to achieve sustainable public transportation in and around University of Kansas campus.

References

1. Hwang, J., et al., *Effect of injection parameters on the combustion and emission characteristics in a common-rail direct injection diesel engine fueled with waste cooking oil biodiesel.* Renewable Energy, 2014. **63**(0): p. 9-17.
2. Hwang, J., et al., *Effect of Injection Parameters on the Combustion and Emission Characteristics in a Compression Ignition Engine Fuelled with Waste Cooking Oil Biodiesel.* 2013, 2013-01-2662, DOI: 10.4271/2013-01-2662.
3. Kannan, G.R. and R. Anand, *Effect of injection pressure and injection timing on DI diesel engine fuelled with biodiesel from waste cooking oil.* Biomass and Bioenergy, 2013. **46**(0): p. 343-352.
4. Langness, C., M. Mangus, and C. Depcik, *Construction, Instrumentation, and Implementation of a Low Cost, Single-Cylinder Compression Ignition Engine Test Cell.* SAE International, 2014, 2014-01-0817, DOI: 10.4271/2014-01-0817.
5. Mangus, M.D., *Design, Construction, and Validation of an In-Cylinder Pressure Recording System for Internal Combustion Engine Analysis.* Department of Mechanical Engineering. Master of Science. 2012. University of Kansas. 1-119.
6. Mangus, M.D., *Implementation of Engine Control and Measurement Strategies for Biofuel Research in Compression-Ignition Engines.* Department of Mechanical Engineering. Doctor of Philosophy. 2014. University of Kansas. 1-526.
7. Langness, C.N., *Effects of Natural Gas Constituents on Engine Performance, Emissions, and Combustion in Compressed Natural Gas-Assisted Diesel Combustion.* Department of Mechanical Engineering. Master of Science. 2014. University of Kansas. 1-384.
8. Cecrle, E., et al., *Investigation of the Effects of Biodiesel Feedstock on the Performance and Emissions of a Single-Cylinder Diesel Engine.* Energy & Fuels, 2012. **26**(4): p. 2331-2341.
9. Mangus, M. and C. Depcik, *Comparison of ULSD, Used Cooking Oil Biodiesel, and JP-8 Performance and Emissions in a Single-Cylinder Compression-Ignition Engine.* SAE International, 2012. **5**(3): p. 1382-1394.2012-32-0009.
10. Mattson, J.M.S., M. Mangus, and C. Depcik, *Efficiency and Emissions Mapping for a Single-Cylinder, Direct Injected Compression Ignition Engine.* SAE International, 2014, 2014-01-1242, DOI: 10.4271/2014-01-1242.
11. Mattson, J.M.S., *Power, Efficiency, and Emissions Optimization of a Single Cylinder Direct-Injected Diesel Engine for Testing of Alternative Fuels through Heat Release Modeling.* Department of Mechanical Engineering. Master of Science. 2013. University of Kansas. 1-187.
12. Zhou, C., et al., *Characteristics and the recovery potential of plastic wastes obtained from landfill mining.* Journal of Cleaner Production, 2014. **80**(0): p. 80-86.
13. Sarkar, M., et al. Waste plastic influence on environment & its solution to create an alternate energy resource. G. Chemistry. 2011.
14. Singhabhandhu, A. and T. Tezuka, *The waste-to-energy framework for integrated multi-waste utilization: Waste cooking oil, waste lubricating oil, and waste plastics.* Energy, 2010. **35**(6): p. 2544-2551.

15. Brebu, M., et al., *Thermal degradation of PE and PS mixed with ABS-Br and debromination of pyrolysis oil by Fe- and Ca-based catalysts.* Polymer Degradation and Stability, 2004. **84**(3): p. 459-467.
16. Al-Salem, S.M., P. Lettieri, and J. Baeyens, *The valorization of plastic solid waste (PSW) by primary to quaternary routes: From re-use to energy and chemicals.* Progress in Energy and Combustion Science, 2010. **36**(1): p. 103-129.
17. Mlynková, B., et al., *Fuels obtained by thermal cracking of individual and mixed polymers.* Chemical Papers, 2010. **64**(1): p. 15-24.
18. Buekens, A.G. and H. Huang, *Catalytic plastics cracking for recovery of gasoline-range hydrocarbons from municipal plastic wastes.* Resources, Conservation and Recycling, 1998. **23**(3): p. 63–181.
19. Walendziewski, J., *Engine fuel derived from wase plastics by thermal treatment.* Fuel, 2002. **81**(4): p. 473-481.
20. Kim, S.-S. and S. Kim, *Pyrolysis characteristics of polystyrene and polypropylene in a stirred batch reactor.* Chemical Engineering Journal, 2004. **98**(1-2): p. 53–60.
21. Panda, A.K. and R.K. Singh, *Catalytic performances of kaoline and silica alumina in the thermal degradation of polypropylene.* Journal of Fuel Chemistry and Technology, 2011. **39**(3): p. 198-202.
22. Jung, S.-H., S.-J. Kim, and J.-S. Kim, *The influence of reaction parameters on characteristics of pyrolysis oils from waste high impact polystyrene and acrylonitrile–butadiene–styrene using a fluidized bed reactor.* Fuel Processing Technology, 2013. **116**(0): p. 123–129.
23. Sharma, B.K., et al., *Production, characterization and fuel properties of alternative diesel fuel from pyrolysis of waste plastic grocery bags.* Fuel Processing Technology, 2014. **122**(0): p. 79–90.
24. Nishino, J., et al., *Catalytic degradation of plastic waste into petrochemicals using Ga-ZSM-5.* Fuel, 2008. **87**(1): p. 3681–3686.
25. Sriningsih, W., et al., *Fuel Production from LDPE Plastic Waste over Natural Zeolite Supported Ni, Ni-Mo, Co and Co-Mo Metals.* Procedia Environmental Sciences, 2014. **20**(1): p. 215-224.
26. Mani, M., G. Nagarajan, and S. Sampath, *Characterisation and effect of using waste plastic oil and diesel fuel blends in compression ignition engine.* Energy, 2011. **36**(1): p. 212-219.
27. Murugan, S., M.C. Ramaswamy, and G. Nagarajan, *The use of tyre pyrolysis oil in diesel engines.* Waste Management, 2008. **28**(12): p. 2743–2749.
28. Kumar, S., et al., *Performance and emission analysis of Blends of WPO.* Energy Conversion and Management, 2013. **74**(0): p. 323–331.
29. Ozcanli, M., *Light and Heavy Phases derived from waste polyethylene by thermal cracking and their usage as fuel in DI diesel engine.* Journal of Scientific & Industrial Research, 2013. **72**(3): p. 198-202.
30. Talens Peiro, L., et al., *Life cycle assessment (LCA) and exergetic life cycle assessment (ELCA) of the production of biodiesel from used cooking oil (UCO).* Energy, 2010. **35**(2): p. 889–893.

31. Mohammadi, P., et al., *Experimental investigation of performance and emission characteristics of DI diesel engine fueled with polymer waste dissolved in biodiesel-blended diesel fuel.* Energy, 2012. **46**(1): p. 596-605.
32. Mania, M., G. Nagarajan, and S. Sampath, *An experimental investigation on a DI diesel engine using waste plastic oil with exhaust gas recirculation.* Fuel, 2010. **89**(1): p. 1826–1832.
33. Murphy, F., et al., *The evaluation of viscosity and density of blends of Cyn-diesel pyrolysis fuel with conventional diesel fuel in relation to compliance with fuel specifications EN 590:2009.* Fuels, 2012. **91**(1): p. 112–118.
34. Energy Systems Division, *Overview on GREET Life Cycle Model*, C.f.T. Research, Editor. 2014, Argonne National Laboratory: https://greet.es.anl.gov/. p. 1-14.
35. Energy Systems Division, *GREET Life Cycle Analysis - User Manual*. 2014, Argonne National Laboratory: https://greet.es.anl.gov/. p. 1-104.
36. Morais, S., et al., *Simulation and life cycle assessment of process design alternatives for biodiesel production from waste vegetable oils.* Journal of Cleaner Production, 2010. **18**(13): p. 1251-1259.
37. Iglesias, L., et al., *A life cycle assessment comparison between centralized and decentralized biodiesel production from raw sunflower oil and waste cooking oils.* Journal of Cleaner Production, 2012. **37**(0): p. 162-171.
38. Tu, Q., C. Zhu, and D.C. McAvoy, *Converting campus waste into renewable energy – A case study for the University of Cincinnati.* Waste Management, 2015. **39**(0): p. 258-265.
39. Varanda, M.G., G. Pinto, and F. Martins, *Life cycle analysis of biodiesel production.* Fuel Processing Technology, 2011. **92**(5): p. 1087–1094.
40. Cao, W., H. Han, and J. Zhang, *Preparation of biodiesel from soybean oil using supercritical methanol and co-solvent.* Fuel, 2005. **84**(4): p. 347-351.
41. Kiwjaroun, C., C. Tubtimdee, and P. Piumsomboon, *LCA studies comparing biodiesel synthesized by conventional and supercritical methanol methods.* Journal of Cleaner Production, 2009. **17**(2): p. 143–153.
42. Pleanjai, S., S.H. Gheewala, and S. Garivait, *Greenhouse gas emissions from production and use of used cooking oil methyl ester as transport fuel in Thailand.* Journal of Cleaner Production, 2009. **17**(9): p. 873-876.
43. Xunmin, O., et al., *Energy consumption and GHG emissions of six biofuel pathways by LCA in (the) People's Republic of China.* Applied Energy, 2009. **86 Supplement 1**(0): p. S197-S208.
44. Yano, J., et al., *Life cycle assessment of hydrogenated biodiesel production from waste cooking oil using the catalytic cracking and hydrogenation method.* Waste Management, 2015. **38**(0): p. 409-423.
45. Mendoza, L.-F.M., et al., *Biodiesel Production from Waste Vegetable Oils: Combining Process Modelling, Multiobjective Optimization and Life Cycle Assessment (LCA).* Computer Aided chemical engineering, 2014. **33**(10): p. 235-240.
46. Pickett, D.K., *Design and Operation of the Synthesis Gas Generator System for Reformed Propane and Glycerin Combustion.* Department of Mechanical Engineering. Master of Science. 2013. University of Kansas. 1-114.

47. Lazarevic, D., et al., *Plastic waste management in the context of a European recycling society: Comparing results and uncertainties in a life cycle perspective.* Resources, Conservation and Recycling, 2010. **55**(2): p. 246-259.
48. Baggio, P., et al., *Energy and environmental analysis of an innovative system based on municipal solid waste (MSW) pyrolysis and combined cycle.* Applied Thermal Engineering, 2008. **28**(2-3): p. 136-144.
49. Astrup, T.F., et al., *Life cycle assessment of thermal Waste-to-Energy technologies: Review and recommendations.* Waste Management, 2015. **37**(0): p. 104-115.
50. Lombardi, L., E. Carnevale, and A. Corti, *A review of technologies and performances of thermal treatment systems for energy recovery from waste.* Waste Management, 2015. **37**(0): p. 26-44.
51. Malkow, T., *Novel and innovative pyrolysis and gasification technologies for energy efficient and environmentally sound MSW disposal.* Waste Management, 2004. **24**(1): p. 53-79.
52. Fodor, Z. and J.r.J. Klemes, *Waste as alternative fuel – Minimising emissions and effluents by advanced design.* Process Safety and Environmental Protection, 2012. **90**(3): p. 263-284.
53. Kumar, S., A.K. Panda, and R.K. Singh, *A review on tertiary recycling of high-density polyethylene to fuel.* Resources, Conservation and Recycling, 2011. **55**(11): p. 893-910.
54. Obeid, F., et al., *Thermo-catalytic pyrolysis of waste polyethylene bottles in a packed bed reactor with different bed materials and catalysts.* Energy Conversion and Management, 2014. **85**(0): p. 1-6.
55. Zeaiter, J., *A process study on the pyrolysis of waste polyethylene.* Fuel, 2014. **133**(0): p. 276-282.
56. Cai, H., et al., *Analysis of Petroleum Refining Energy Efficiency of U.S. Refineries*, S.N.A. Inc, Editor. 2013, Argonne National Laboratory. p. 1-16.
57. Palou-Rivera, I., J. Han, and M. Wang, *Updates to Petroleum Refining and Upstream Emissions*, in *Center for Transportation Research*. 2011, Argonne National Laboratory. p. 1-12.
58. Mangus, M., et al., *Comparison of Neat Biodiesels and ULSD in an Optimized Single-Cylinder Diesel Engine with Electronically-Controlled Fuel Injection.* Energy & Fuels, 2014. **28**(6): p. 3849-3862.
59. Ganapathy, T., R.P. Gakkhar, and K. Murugesan, *Influence of injection timing on performance, combustion and emission characteristics of Jatropha biodiesel engine.* Applied Energy, 2011. **88**(12): p. 4376-4386.
60. Dhananjaya, D.A., P. Mohanan, and C.V. Sudhir, *Effect of Injection Pressure and Injection Timing on a Semi-Adiabatic CI Engine Fueled With Blends of Jatropha Oil Methyl Esters.* 2008, DOI: 10.4271/2008-28-0070.
61. Pandian, M., S.P. Sivapirakasam, and M. Udayakumar, *Investigation on the effect of injection system parameters on performance and emission characteristics of a twin cylinder compression ignition direct injection engine fuelled with pongamia biodiesel–diesel blend using response surface methodology.* Applied Energy, 2011. **88**(8): p. 2663-2676.

62. Basavaraja, T. and R.R. Prathap, *Effect of Injection Pressure on Emission Performance of Bio-diesel and its Blends.* 2005.
63. Gumus, M., C. Sayin, and M. Canakci, *The impact of fuel injection pressure on the exhaust emissions of a direct injection diesel engine fueled with biodiesel–diesel fuel blends.* Fuel, 2012. **95**(0): p. 486-494.
64. Jaichandar, S. and K. Annamalai, *Combined impact of injection pressure and combustion chamber geometry on the performance of a biodiesel fueled diesel engine.* Energy, 2013. **55**(0): p. 330-339.
65. Qi, D., C.-F. Lee, and Y. Lin, *Effect of Injection Parameters and EGR on the Particle Size Distributions and Exhaust Emissions for Diesel and Biodiesel Fuels in CRDI Engine.* 2014, 2014-01-1612, DOI: 10.4271/2014-01-1612.
66. Mito, Y., et al., *The Effect of Intake, Injection Parameters and Fuel Properties on Diesel Combustion and Emissions.* 2003, 2003-01-1793, DOI: 10.4271/2003-01-1793.
67. Hariprasad, T., *Effect of Injection Pressure on Performance of Dual Fuel Diesel Engine.* SAE International, 2013, 2013-01-2887, DOI: 10.4271/2013-01-2887.
68. Mather, D.K. and R.D. Reitz, *Modelling the Influence of Fuel Injection Parameters on Diesel Engine Emissions.* SAE International, 1998, 980789, DOI: 10.4271/980789.
69. Alptekin, E. and M. Canakci, *Determination of the density and the viscosities of biodiesel– diesel fuel blends.* Renewable Energy, 2008. **33**(12): p. 2623-2630.
70. Mangus, M., et al., *Investigating the Compression Ignition Combustion of Multiple Biodiesel/ULSD Blends via Common-Rail Injection.* Energy, 2015(in press).
71. Mattson, J.M.S. and C. Depcik, *Emissions–calibrated equilibrium heat release model for direct injection compression ignition engines.* Fuel, 2014. **117, Part B**(0): p. 1096-1110.
72. Mattson, J., E. Reznicek, and C. Depcik. *Second Law Heat Release Model of a Compression Ignition Engine*. ASME. 2015. IMECE2015-51079. under review.